NIST SPECIAL PUBLICATION 260-117

U.S. DEPARTMENT OF COMMERCE/Technology Administration/National Institute of Standards and Technology

Standard Reference Materials:

Antireflecting-Chromium Linewidth Standard, SRM 475, for Calibration of Optical Microscope Linewidth Measuring Systems

Carol F. Vezzetti, Ruth N. Varner, and James E. Potzick

NIST Special Publication 260-117

Standard Reference Materials:

Antireflecting-Chromium Linewidth Standard, SRM 475, for Calibration of Optical Microscope Linewidth Measuring Systems

Carol F. Vezzetti
Ruth N. Varner
James E. Potzick

Precision Engineering Division
Manufacturing Engineering Laboratory
National Institute of Standards and Technology
Gaithersburg, MD 20899

U.S. DEPARTMENT OF COMMERCE, Robert A. Mosbacher, Secretary
TECHNOLOGY ADMINISTRATION, Robert M. White, Under Secretary for Technology
NATIONAL INSTITUTE OF STANDARDS AND TECHNOLOGY, John W. Lyons, Director

Issued January 1992

National Institute of Standards and Technology Special Publication 260-117
Natl. Inst. Stand. Technol. Spec. Publ. 260-117, 49 pages (Jan. 1992)
CODEN: NSPUE2

U.S. GOVERNMENT PRINTING OFFICE
WASHINGTON: 1992

For sale by the Superintendent of Documents, U.S. Government Printing Office, Washington, DC 20402-9325

Preface

Standard Reference Materials (SRM's) as defined by the National Institute of Standards and Technology (NIST) are well-characterized materials, produced in quantity and certified for one or more physical or chemical properties. They are used to assure the accuracy and compatibility of measurements throughout the Nation. SRM's are widely used as primary standards in many diverse fields in science, industry, and technology, both within the United States and throughout the world. They are also used extensively in the fields of environmental and clinical analysis. In many applications, traceability of quality control and measurement processes to the national measurement system is carried out through the mechanism and use of SRM's. For many of the Nation's scientists and technologists, it is therefore of more than passing interest to know the details of the measurements made at NIST in arriving at the certified values of the SRM's produced. The NIST Special Publication 260 Series is a series of papers reserved for this purpose.

The 260 Series is dedicated to the dissemination of information on different phases of the preparation, measurement, certification, and use of NIST SRM's. In general, much more detail will be found in these papers than is generally allowed, or desirable, in scientific journal articles. This enables the user to assess the validity and accuracy of the measurement processes employed, to judge the statistical analysis, and to learn details of techniques and methods utilized for work entailing greatest care and accuracy. These papers also should provide sufficient additional information so SRM's can be utilized in new applications in diverse fields not foreseen at the time the SRM was originally issued.

Inquiries concerning the technical content of this paper should be directed to the author(s). Other questions concerned with the availability, delivery, price, and so forth, will receive prompt attention from:

Standard Reference Materials Program
Bldg. 202, Rm. 204
National Institute of Standards and Technology
Gaithersburg, MD 20899

William P. Reed, Chief
Standard Reference Materials Program

OTHER NIST PUBLICATIONS IN THIS SERIES

McKenzie, R. L., ed., NIST Standard Reference Materials Catalog 1990-91, NIST Spec. Publ. 260 (January 1990)

Michaelis, R. E., and Wyman, L. L., Standard Reference Materials: Preparation of White Cast Iron Spectrochemical Standards, NBS Misc. Publ. 260-1 (June 1964). COM74-11061**

Michaelis, R. E., Wyman, L. L., and Flitsch, R., Standard Reference Materials: Preparation of NBS Copper-Base Spectrochemical Standards, NBS Misc. Publ. 260-2 (October 1964). COM74-11063**

Michaelis, R. E., Yakowitz, H., and Moore, G. A., Standard Reference Materials: Metallographic Characterization of an NBS Spectrometric Low-Alloy Steel Standard, NBS Misc. Publ. 260-3 (October 1964). COM74-11060**

Alvarez, R., and Flitsch, R., Standard Reference Materials: Accuracy of Solution X-Ray Spectrometric Analysis of Copper-Base Alloys, NBS Misc. Publ. 260-5 (March 1965). PB168068**

Shultz, J. I., Standard Reference Materials: Methods for the Chemical Analysis of White Cast Iron Standards, NBS Misc. Publ. 260-6 (July 1965). COM74-11068**

Bell, R. K., Standard Reference Materials: Methods for the Chemical Analysis of NBS Copper-Base Spectrochemical Standards, NBS Misc. Publ. 260-7 (October 1965). COM74-11067**

Richmond, M. S., Standard Reference Materials: Analysis of Uranium Concentrates at the National Bureau of Standards, NBS Misc. Publ. 260-8 (December 1965). COM74-11066**

Anspach, S. C., Cavallo, L. M., Garfinkel, S. B., Hutchinson, J. M. R., and Smith, C. N., Standard Reference Materials: Half Lives of Materials Used in the Preparation of Standard Reference Materials of Nineteen Radioactive Nuclides Issued by the National Bureau of Standards, NBS Misc. Publ. 260-9 (November 1965). COM74-11065**

Yakowitz, H., Vieth, D. L., Heinrich, K. F. J., and Michaelis, R. E., Standard Reference Materials: Homogeneity Characterization of NBS Spectrometric Standards II: Cartridge Brass and Low-Alloy Steel, NBS Misc. Publ. 260-10 (December 1965). COM74-11064**

Napolitano, A., and Hawkins, E. G., Standard Reference Materials: Viscosity of Standard Lead-Silica Glass, NBS Misc. Publ. 260-11 (November 1966).

Yakowitz, H., Vieth, D. L., and Michaelis, R. E., Standard Reference Materials: Homogeneity Characterization of NBS Spectrometric Standards III: White Cast Iron and Stainless Steel Powder Compact, NBS Misc. Publ. 260-12 (September 1966).

Menis, O., and Sterling, J. T., Standard Reference Materials: Determination of Oxygen in Ferrous Materials—SRM 1090, 1091, and 1092, NBS Misc. Publ. 260-14 (September 1966).

Yakowitz, H., Michaelis, R. E., and Vieth, D. L., Standard Reference Materials: Homogeneity Characterization of NBS Spectrometric Standards IV: Preparation and Microprobe Characterization of W-20% Mo Alloy Fabricated by Powder Metallurgical Methods, NBS Spec. Publ. 260-16 (January 1969). COM74-11062**

Paule, R. C., and Mandel, J., Standard Reference Materials: Analysis of Interlaboratory Measurements on the Vapor Pressure of Gold (Certification of Standard Reference Material 745). NBS Spec. Publ. 260-19 (January 1970). PB190071**

Paule, R. C., and Mandel, J., Standard Reference Materials: Analysis of Interlaboratory Measurements on the Vapor Pressures of Cadmium and Silver, NBS Spec. Publ. 260-21 (January 1971). COM74-11359**

Yakowitz, H., Fiori, C. E., and Michaelis, R. E., Standard Reference Materials: Homogeneity Characterization of Fe-3 Si Alloy, NBS Spec. Publ. 260-22 (February 1971). COM74-11357**

Napolitano, A., and Hawkins, E. G., Standard Reference Materials: Viscosity of a Standard Borosilicate Glass, NBS Spec. Publ. 260-23 (December 1970). COM71-00157**

Sappenfield, K. M., Marinenko, G., and Hague, J. L., Standard Reference Materials: Comparison of Redox Standards, NBS Spec. Publ. 260-24 (January 1972). COM72-50058**

Hicho, G. E., Yakowitz, H., Rasberry, S. D., and Michaelis, R. E., Standard Reference Materials: A Standard Reference Material Containing Nominally Four Percent Austenite, NBS Spec. Publ. 260-25 (February 1971). COM74-11356**

Martin, J. F., Standard Reference Materials: National Bureau of Standards-US Steel Corporation Joint Program for Determining Oxygen and Nitrogen in Steel, NBS Spec. Publ. 260-26 (February 1971). PB 81176620**

Garner, E. L., Machlan, L. A., and Shields, W. R., Standard Reference Materials: Uranium Isotopic Standard Reference Materials, NBS Spec. Publ. 260-27 (April 1971). COM74-11358**

Heinrich, K. F. J., Myklebust, R. L., Rasberry, S. D., and Michaelis, R. E., Standard Reference Materials: Preparation and Evaluation of SRM's 481 and 482 Gold-Silver and Gold-Copper Alloys for Microanalysis, NBS Spec. Publ. 260-28 (August 1971). COM71-50365**

Geller, S. B., Standard Reference Materials: Calibration of NBS Secondary Standard Magnetic Tape (Computer Amplitude Reference) Using the Reference Tape Amplitude Measurement "Process A-Model 2," NBS Spec. Publ. 260-29 (June 1971). COM71-50282**

Gorozhanina, R. S., Freedman, A. Y., and Shaievitch, A. B. (translated by M. C. Selby), Standard Reference Materials: Standard Samples Issued in the USSR (A Translation from the Russian), NBS Spec. Publ. 260-30 (June 1971). COM71-50283**

Hust, J. G., and Sparks, L. L., Standard Reference Materials: Thermal Conductivity of Electrolytic Iron SRM 734 from 4 to 300 K, NBS Spec. Publ. 260-31 (November 1971). COM71-50563**

Mavrodineanu, R., and Lazar, J. W., Standard Reference Materials: Standard Quartz Cuvettes for High Accuracy Spectrophotometry, NBS Spec. Publ. 260-32 (December 1973). COM74-50018**

Wagner, H. L., Standard Reference Materials: Comparison of Original and Supplemental SRM 705, Narrow Molecular Weight Distribution Polystyrene, NBS Spec. Publ. 260-33 (May 1972). COM72-50526**

Sparks, L. L., and Hust, J. G., Standard Reference Materials: Thermal Conductivity of Austenitic Stainless Steel, SRM 735 from 5 to 280 K, NBS Spec. Publ. 260-35 (April 1972.) COM72-50368**

Cali, J. P., Mandel, J., Moore, L. J., and Young, D. S., Standard Reference Materials: A Referee Method for the Determination of Calcium in Serum NBS SRM 915, NBS Spec. Publ. 260-36 (May 1972). COM72-50527**

Shultz, J. I., Bell, R. K., Rains, T. C., and Menis, O., Standard Reference Materials: Methods of Analysis of NBS Clay Standards, NBS Spec. Publ. 260-37 (June 1972). COM72-50692**

Clark, A. F., Denson, V. A., Hust, J. G., and Powell, R. L., Standard Reference Materials: The Eddy Current Decay Method for Resistivity Characterization of High-Purity Metals, NBS Spec. Publ. 260-39 (May 1972). COM72-50529**

McAdie, H. G., Garn, P. D., and Menis, O., Standard Reference Materials: Selection of Thermal Analysis Temperature Standards Through a Cooperative Study (SRM 758, 759, 760), NBS Spec. Publ. 260-40 (August 1972) COM72-50776**

Wagner, H. L., and Verdier, P. H., eds., Standard Reference Materials: The Characterization of Linear Polyethylene, SRM 1475, NBS Spec. Publ. 260-42 (September 1972). COM72-50944**

Yakowitz, H., Ruff, A. W., and Michaelis, R. E., Standard Reference Materials: Preparation and Homogeneity Characterization of an Austenitic Iron-Chromium-Nickel Alloy, NBS Spec. Publ. 260-43 (November 1972). COM73-50760**

Schooley, J. F., Soulen, R. J., Jr., and Evans, G. A., Jr., Standard Reference Materials: Preparation and Use of Superconductive Fixed Point Devices, SRM 767, NBS Spec. Publ. 260-44 (December 1972). COM73-50037**

Greifer, B., Maienthal, E. J., Rains, T. C., and Rasberry, S. D., Standard Reference Materials: Powdered Lead-Based Paint, SRM 1579, NBS Spec. Publ. 260-45 (March 1973). COM73-50226**

Hust, J. G., and Giarratano, P. J., Standard Reference Materials: Thermal Conductivity and Electrical Resistivity Standard Reference Materials: Austenitic Stainless Steel, SRM's 735 and 798, from 4 to 1200 K, NBS Spec. Publ. 260-46 (March 1975). COM75-10339**

Hust, J. G., Standard Reference Materials: Electrical Resistivity of Electrolytic Iron, SRM 797, and Austenitic Stainless Steel, SRM 798, from 5 to 280 K, NBS Spec. Publ. 260-47 (February 1974). COM74-50176**

Mangum, B. W., and Wise, J. A., Standard Reference Materials: Description and Use of Precision Thermometers for the Clinical Laboratory, SRM 933 and SRM 934, NBS Spec. Publ. 260-48 (May 1974). Superseded by NIST Spec. Publ. 260-113.

Carpenter, B. S., and Reimer, G. M., Standard Reference Materials: Calibrated Glass Standards for Fission Track Use, NBS Spec. Publ. 260-49 (November 1974). COM74-51185**

Hust, J. G., and Giarratano, P. J., Standard Reference Materials: Thermal Conductivity and Electrical Resistivity Standard Reference Materials: Electrolytic Iron, SRM's 734 and 797 from 4 to 1000 K, NBS Spec. Publ. 260-50 (June 1975). COM75-10698**

Mavrodineanu, R., and Baldwin, J. R., Standard Reference Materials: Glass Filters As a Standard Reference Material for Spectrophotometry-Selection, Preparation, Certification, Use-SRM 930 NBS Spec. Publ. 260-51 (November 1975). COM75-10339**

Hust, J. G., and Giarratano, P. J., Standard Reference Materials: Thermal Conductivity and Electrical Resistivity Standard Reference Materials 730 and 799, from 4 to 3000 K, NBS Spec. Publ. 260-52 (September 1975). COM75-11193**

Durst, R. A., Standard Reference Materials: Standardization of pH Measurements, NBS Spec. Publ. 260-53 (February 1988, Revision of December 1975 version).

Burke, R. W., and Mavrodineanu, R., Standard Reference Materials: Certification and Use of Acidic Potassium Dichromate Solutions as an Ultraviolet Absorbance Standard, NBS Spec. Publ. 260-54 (August 1977). PB272168**

Ditmars, D. A., Cezairliyan, A., Ishihara, S., and Douglas, T. B., Standard Reference Materials: Enthalpy and Heat Capacity; Molybdenum SRM 781, from 273 to 2800 K, NBS Spec. Publ. 260-55 (September 1977). PB272127**

Powell, R. L., Sparks, L. L., and Hust, J. G., Standard Reference Materials: Standard Thermocouple Material, Pt-67: SRM 1967, NBS Spec. Publ. 260-56 (February 1978). PB277172**

Barnes, J. D., and Martin, G. M., Standard Reference Materials: Polyester Film for Oxygen Gas Transmission Measurements SRM 1470, NBS Spec. Publ. 260-58 (June 1979). PB297098**

Velapoldi, R. A., Paule, R. C., Schaffer, R., Mandel, J., and Moody, J. R., Standard Reference Materials: A Reference Method for the Determination of Sodium in Serum, NBS Spec. Publ. 260-60 (August 1978). PB286944**

Verdier, P H., and Wagner, H. L., Standard Reference Materials: The Characterization of Linear Polyethylene (SRM 1482, 1483, 1484), NBS Spec. Publ. 260-61 (December 1978). PB289899**

Soulen, R. J., and Dove, R. B., Standard Reference Materials: Temperature Reference Standard for Use Below 0.5 K (SRM 768), NBS Spec. Publ. 260-62 (April 1979). PB294245**

Velapoldi, R. A., Paule, R. C., Schaffer, R., Mandel, J., Machlan, L. A., and Gramlich, J. W., Standard Reference Materials: A Reference Method for the Determination of Potassium in Serum, NBS Spec. Publ. 260-63 (May 1979). PB297207**

Velapoldi, R. A., and Mielenz, K. D., Standard Reference Materials: A Fluorescence Standard Reference Material Quinine Sulfate Dihydrate (SRM 936), NBS Spec. Publ. 260-64 (January 1980). PB80-132046**

Marinenko, R. B., Heinrich, K. F. J., and Ruegg, F. C., Standard Reference Materials: Micro-Homogeneity Studies of NBS Standard Reference Materials, NBS Research Materials, and Other Related Samples, NBS Spec. Publ. 260-65 (September 1979). PB300461**

Venable, W. H., Jr., and Eckerle, K. L., Standard Reference Materials: Didymium Glass Filters for Calibrating the Wavelength Scale of Spectrophotometers-SRM 2009, 2010, 2013, and 2014, NBS Spec. Publ. 260-66 (October 1979). PB80-104961**

Velapoldi, R. A., Paule, R. C., Schaffer, R., Mandel, J., Murphy, T. J., and Gramlich, J. W., Standard Reference Materials: A Reference Method for the Determination of Chloride in Serum, NBS Spec. Publ. 260-67 (November 1979). PB80-110117**

Mavrodineanu, R., and Baldwin, J. R., Standard Reference Materials: Metal-On-Quartz Filters as a Standard Reference Material for Spectrophotometry SRM 2031, NBS Spec. Publ. 260-68 (April 1980). PB80-197486**

Velapoldi, R. A., Paule, R. C., Schaffer, R., Mandel, J., Machlan, L. A., Garner, E. L., and Rains, T. C., Standard Reference Materials: A Reference Method for the Determination of Lithium in Serum, NBS Spec. Publ. 260-69 (July 1980). PB80-209117**

Marinenko, R. B., Biancaniello, F., Boyer, P. A., Ruff, A. W., and DeRobertis, L., Standard Reference Materials: Preparation and Characterization of an Iron-Chromium-Nickel Alloy for Microanalysis, NBS Spec. Publ. 260-70 (May 1981). PB84-165349**

Seward, R. W., and Mavrodineanu, R., Standard Reference Materials: Summary of the Clinical Laboratory Standards Issued by the National Bureau of Standards, NBS Spec. Publ. 260-71 (November 1981). PB82-135161**

Reeder, D. J., Coxon, B., Enagonio, D., Christensen, R. G., Schaffer, R., Howell, B. F., Paule, R. C., and Mandel, J., Standard Reference Materials: SRM 900, Antiepilepsy Drug Level Assay Standard, NBS Spec. Publ. 260-72 (June 1981). PB81-220758

Interrante, C. G., and Hicho, G. E., Standard Reference Materials: A Standard Reference Material Containing Nominally Fifteen Percent Austenite (SRM 486), NBS Spec. Publ. 260-73 (January 1982). PB82-215559**

Marinenko, R. B., Standard Reference Materials: Preparation and Characterization of K-411 and K-414 Mineral Glasses for Microanalysis: SRM 470, NBS Spec. Publ. 260-74 (April 1982). PB82-221300**

Weidner, V. R., and Hsia, J. J., Standard Reference Materials: Preparation and Calibration of First Surface Aluminum Mirror Specular Reflectance Standards (SRM 2003a), NBS Spec. Publ. 260-75 (May 1982). PB82-221367**

Hicho, G. E., and Eaton, E. E., Standard Reference Materials: A Standard Reference Material Containing Nominally Five Percent Austenite (SRM 485a), NBS Spec. Publ. 260-76 (August 1982). PB83-115568**

Furukawa, G. T., Riddle, J. L., Bigge, W. G., and Pfieffer, E. R., Standard Reference Materials: Application of Some Metal SRM's as Thermometric Fixed Points, NBS Spec. Publ. 260-77 (August 1982). PB83-117325**

Hicho, G. E., and Eaton, E. E., Standard Reference Materials: Standard Reference Material Containing Nominally Thirty Percent Austenite (SRM 487), NBS Spec. Publ. 260-78 (September 1982). PB83-115576**

Richmond, J. C., Hsia, J. J., Weidner, V. R., and Wilmering, D. B., Standard Reference Materials: Second Surface Mirror Standards of Specular Spectral Reflectance (SRM's 2023, 2024, 2025), NBS Spec. Publ. 260-79 (October 1982). PB84-203447**

Schaffer, R., Mandel, J., Sun, T., Cohen, A., and Hertz, H. S., Standard Reference Materials: Evaluation by an ID/MS Method of the AACC Reference Method for Serum Glucose, NBS Spec. Publ. 260-80 (October 1982). PB84-216894**

Burke, R. W., and Mavrodineanu, R., Standard Reference Materials: Accuracy in Analytical Spectrophotometry, NBS Spec. Publ. 260-81 (April 1983). PB83-214536**

Weidner, V. R., Standard Reference Materials: White Opal Glass Diffuse Spectral Reflectance Standards for the Visible Spectrum (SRM's 2015 and 2016), NBS Spec. Publ. 260-82 (April 1983). PB83-220723**

Bowers, G. N., Jr., Alvarez, R., Cali, J. P., Eberhardt, K. R., Reeder, D. J., Schaffer, R., and Uriano, G. A., Standard Reference Materials: The Measurement of the Catalytic (Activity) Concentration of Seven Enzymes in NBS Human Serum SRM 909, NBS Spec. Publ. 260-83 (June 1983). PB83-239509**

Gills, T. E., Seward, R. W., Collins, R. J., and Webster, W. C., Standard Reference Materials: Sampling, Materials Handling, Processing, and Packaging of NBS Sulfur in Coal Standard Reference Materials 2682, 2683, 2684, and 2685, NBS Spec. Publ. 260-84 (August 1983). PB84-109552**

Swyt, D. A., Standard Reference Materials: A Look at Techniques for the Dimensional Calibration of Standard Microscopic Particles, NBS Spec. Publ. 260-85 (September 1983). PB84-112648**

Hicho, G. E., and Eaton, E. E., Standard Reference Materials: A Standard Reference Material Containing Two and One-Half Percent Austenite, SRM 488, NBS Spec. Publ. 260-86 (December 1983). PB84-143296**

Mangum, B. W., Standard Reference Materials: SRM 1969: Rubidium Triple-Point - A Temperature Reference Standard Near 39.30 °C, NBS Spec. Publ. 260-87 (December 1983). PB84-149996**

Gladney, E. S., Burns, C. E., Perrin, D. R., Roelandts, I., and Gills, T. E., Standard Reference Materials: 1982 Compilation of Elemental Concentration Data for NBS Biological, Geological, and Environmental Standard Reference Materials, NBS Spec. Publ. 260-88 (March 1984). PB84-218338**

Hust, J. G., Standard Reference Materials: A Fine-Grained, Isotropic Graphite for Use as NBS Thermophysical Property RM's from 5 to 2500 K, NBS Spec. Publ. 260-89 (September 1984). PB85-112886**

Hust, J. G., and Lankford, A. B., Standard Reference Materials: Update of Thermal Conductivity and Electrical Resistivity of Eleetrolytic Iron, Tungsten, and Stainless Steel, NBS Spec. Publ. 260-90 (September 1984). PB85-115814**

Goodrich, L. F., Vecchia, D. F., Pittman, E. S., Ekin, J. W., and Clark, A. F., Standard Reference Materials: Critical Current Measurements on an NbTi Superconducting Wire Standard Reference Material, NBS Spec. Publ. 260-91 (September 1984). PB85-118594**

Carpenter, B. S., Standard Reference Materials: Calibrated Glass Standards for Fission Track Use (Supplement to NBS Spec. Publ. 260-49), NBS Spec. Publ. 260-92 (September 1984). PB85-113025**

Ehrstein, J.R., Standard Reference Materials: Preparation and Certification of Standard Reference Materials for Calibration of Spreading Resistance Probes, NBS Spec. Publ. 260-93 (January 1985). PB85-177921**

Gills, T. E., Koch, W. F., Stolz, J. W., Kelly, W. R., Paulsen, P. J., Colbert, J. C., Kirklin, D. R., Pei, P.T.S., Weeks, S., Lindstrom, R. M., Fleming, R. F., Greenberg, R. R., and Paule, R. C., Standard Reference Materials: Methods and Procedures Used at the National Bureau of Standards to Certify Sulfur in Coal SRM's for Sulfur Content, Calorific Value, Ash Content, NBS Spec. Publ. 260-94 (December 1984). PB85-165900**

Mulholland, G. W., Hartman, A. W., Hembree, G. G., Marx, E., and Lettieri, T. R., Standard Reference Materials: Development of a 1 μm Diameter Particle Size Standard, SRM 1690, NBS Spec. Publ. 260-95 (May 1985). SN003-003-02665-4*

Carpenter, B. S., Gramlich, J. W., Greenberg, R. R., Machlan, L. A., DeBievre, P., Eschbach, H. L., Meyer, H., Van Audenhove, J., Connolly, V. E., Trahey, N. M., and Zook, A. C., Standard Reference Materials: Uranium-235 Isotopic Abundance Standard Reference Materials for Gamma Spectrometry Measurements, NBS Spec. Publ. 260-96 (September 1986). PB87-108544**

Mavrodineanu, R., and Gills, T. E., Standard Reference Materials: Summary of the Coal, Ore, Mineral, Rock, and Refactory Standards Issued by the National Bureau of Standards, NBS Spec. Publ. 260-97 (September 1985). SN003-003-02688-3*

Hust, J. G., Standard Reference Materials: Glass Fiberboard SRM for Thermal Resistance, NBS Spec. Publ. 260-98 (August 1985). SN003-003-02674-3*

Callanan, J. E., Sullivan, S. A., and Vecchia, D. F., Standard Reference Materials: Feasibility Study for the Development of Standards Using Differential Scanning Calorimetry, NBS Spec. Publ. 260-99 (August 1985). SN003-003-02675-1*

Taylor, J. K., Standard Reference Materials: Handbook for SRM Users, NBS Spec. Publ. 260-100 (September 1985). PB86-110897**

Mangum, B. W., Standard Reference Materials: SRM 1970, Succinonitrile Triple-Point Standard: A Temperature Reference Standard Near 58.08 °C, NBS Spec. Publ. 260-101 (March 1986). SN003-003-02722-7*

Weidner, V. R., Mavrodineanu, R., Mielenz, K. D., Velapoldi, R. A., Eckerle, K. L., and Adams, B., Standard Reference Materials: Holmium Oxide Solution Wavelength Standard from 240 to 640 nm - SRM 2034, NBS Spec. Publ. 260-102 (July 1986). PB86-245727**

Hust, J. G., Standard Reference Materials: Glass Fiberblanket SRM for Thermal Resistance, NBS Spec. Publ. 260-103 (September 1985). SN003-003-02687-5*

Mavrodineanu, R., and Alvarez, R., Standard Reference Materials: Summary of the Biological and Botanical Standards Issued by the National Bureau of Standards, NBS Spec. Publ. 260-104 (November 1985). SN003-003-02704-9*

Mavrodineanu, R., and Rasberry, S. D., Standard Reference Materials: Summary of the Environmental Research, Analysis, and Control Standards Issued by the National Bureau of Standards, NBS Spec. Publ. 260-105 (March 1986). SN003-003-02725-1*

Koch, W. F., ed., Standard Reference Materials: Methods and Procedures Used at the National Bureau of Standards to Prepare, Analyze, and Certify SRM 2694, Simulated Rainwater, and Recommendations for Use, NBS Spec. Publ. 260-106 (July 1986). PB86-247483**

Hartman, A. W., and McKenzie, R. L., Standard Reference Materials: SRM 1965, Microsphere Slide (10 μm Polystyrene Spheres), NBS Spec. Publ. 260-107 (November 1988).

Mavrodineanu, R., and Gills, T. E., Standard Reference Materials: Summary of Gas Cylinder and Permeation Tube Standard Reference Materials Issued by the National Bureau of Standards, NBS Spec. Publ. 260-108 (May 1987).

Candela, G. A., Chandler-Horowitz, D., Novotny, D. B., Marchiando, J. F., and Belzer, B. J., Standard Reference Materials: Preparation and Certification of an Ellipsometrically Derived Thickness and Refractive Index Standard of a Silicon Dioxide Film (SRM 2530), NIST Spec. Publ. 260-109 (October 1988).

Kirby, R. K., and Kanare, H. M., Standard Reference Materials: Portland Cement Chemical Composition Standards (Blending, Packaging, and Testing), NBS Spec. Publ. 260-110 (February 1988).

Gladney, E. S., O'Malley, B. T., Roelandts, I., and Gills, T. E., Standard Reference Materials: Compilation of Elemental Concentration Data for NBS Clinical, Biological, Geological, and Environmental Standard Reference Materials, NBS Spec. Publ. 260-111 (November 1987).

Marinenko, R. B., Blackburn, D. H., and Bodkin, J. B., Standard Reference Materials: Glasses for Microanalysis: SRM's 1871-1875, NIST Spec. Publ. 260-112 (February 1990).

Mangum, B. W., and Wise, J. A., Standard Reference Materials: Description and Use of a Precision Thermometer for the Clinical Laboratory, SRM934, NIST Spec. Publ. 260-113 (June 1990).

Vezzetti, C. F., Varner, R. N. and Potzick, J. E., Standard Reference Materials: Bright-Chromium Linewidth Standard, SRM 476, for Calibration of Optical Microscope Linewidth Measuring Systems, NIST Spec. Publ. 260-114 (January 1991).

Williamson, M. P., Willman, N. E., and Grubb, D. S., Standard Reference Materials: Calibration of NIST Standard Reference Material 3201 for 0.5 Inch (12.65 mm) Serial Serpentine Magnetic Tape Cartridge, NIST Spec. Publ. 260-115 (February 1991).

Mavrodineanu, R. , Burke, R. W., Baldwin, J. R., Smith, M. V., and Messman, J. D., Standard Reference Materials: Glass Filters as a Standard Reference Material for Spectrophotometry and Selection, Preparation, Certification and use of SRM 930 and SRM 1930, NIST Spec. Publ. 260-116 (in prep).

*Send order with remittance to Superintendent of Documents, U.S. Government Printing Office, Washington, DC 20102. Remittance from foreign countries should include an additional one fourth of the purchase price for postage.

**May be ordered from: National Technical Information Services (NTIS), Springfield, VA 22161.

Contents

ANTIREFLECTING-CHROMIUM LINEWIDTH STANDARD, SRM 475, FOR CALIBRATION OF OPTICAL MICROSCOPE LINEWIDTH MEASURING SYSTEMS

C. F. Vezzetti, R. N. Varner, and J. E. Potzick

National Institute of Standards and Technology
Gaithersburg, Maryland 20899

ABSTRACT

The precise and accurate measurement of feature dimensions on photomasks, such as those used in the production of integrated circuits, becomes increasingly difficult as the dimensions approach the wavelength of the light used to make the measurement. The undesirable effects of optical diffraction obsure the location of the feature edges. Raggedness and non-vertical walls along the edges add to the uncertainty of the measurement.

Standard Reference Material SRM 475 was developed for use in calibrating optical microscopes for measuring linewidths in the range of 0.9 to 10.8 μm on antireflecting-chromium photomasks. The SRM, the measurement system, and the procedures used to calibrate the SRM are described. The algorithm for determining the line edge location uses a threshold criterion derived from analysis of microscope image profiles. The profiles are predicted by computer modeling based on the theory of partial coherence. The performance of the system is monitored by measuring line features on a control photomask before and after calibrating each SRM.

Precautions concerning care and handling and instruction for the use of SRM 475 to calibrate optical microscopes for photomask linewidth measurement are given.

KEY WORDS: accuracy; antireflecting-chromium; calibration; control charts; critical dimensions; integrated circuits; linewidth measurement; optical microscope; photomask; precision; semiconductor industry; standard reference material; statistical process control; threshold; uncertainty.

1. Introduction

The ability to measure and control critical dimensions during the production of integrated circuits is essential to the semiconductor industry. Many measuring systems claiming high precision are now commercially available for measuring some of these critical dimensions. As part of a continuing effort to provide means for calibrating these systems, the National Institute of Standards and Technology (NIST) has developed Optical Microscope Linewidth Measurement Standard Reference Materials.

Standard Reference Material (SRM) 475 is designed for calibrating optical microscope systems to measure linewidths on antireflecting-chromium photomasks. It was produced with conventional technology by a commercial photomask manufacturing facility. In addition to isolated opaque and clear lines for linewidth calibration, this SRM contains line patterns for checking length scale, adjusting video-type micrometers, and detecting mechanical or optical nonlinearities. The design of the calibrated pattern is described in section 2.

A photometric microscope with lenses selected for least aberration was modified at NIST for calibrating the SRM line features with green light illumination of wavelength 0.53 μm. Except for the initial positioning, aligning, and focusing of the photomask, the entire calibration process is automated. Linewidths are determined from the image profile (image intensity versus position across a feature) based on a considerable amount of theoretical work conducted to establish the location on the observed image profile that corresponds to the physical edge of a feature. The quality of the feature edge geometry of a sample from each production batch of SRM photomasks is examined with a scanning electron microscope (SEM). The limit of accuracy of the calibration measurements given in the certificate data is based on this sampled edge geometry and the agreement between theoretically modeled and experimentally generated image profiles. Section 3 contains brief descriptions of the NIST linewidth calibration system and the automated calibration process as well as discussions of the line edge location algorithm, precision, and accuracy.

Section 4 gives information and precautions on the care and use of this SRM to calibrate an optical linewidth measuring system. Because of the variety of linewidth measurement systems in use today, no attempt has been made to give specific instructions for each type of microscope.

The process control procedures used in the calibration of this SRM are discussed in some detail in the Appendix.

2. Physical Characteristics of SRM 475

SRM 475 is made from an antireflecting-chromium photoplate by conventional photolithographic techniques. The substrate is a quartz plate of a type commonly used for fabricating integrated circuit photomasks, nominally 63.5 x 63.5 x 1.5 mm (2.5 x 2.5 x 0.060 in). The nominal thickness of the chromium layer is 100 nm.

Figure 1 shows the overall pattern on the chromium-coated side of the standard. The cross-shaped relatively clear area contains a series of horizontal and vertical lines that are used to help locate the basic measurement pattern which is repeated at eight locations around the center of the standard as shown in figure 2 (a magnified view of central area of fig. 1). A pattern identification number (1 through 8) is located to the left of each basic pattern. Only one of these eight patterns is certified by NIST; it is identified on the accompanying certificate.

Figure 3 shows the details of the features in each of the eight identical patterns on the SRM. Letters A, B, E, F, and G designate the row locations, and numbers 0 through 9 designate column locations. Thus, each feature can be identified by its row and column coordinates; for example, A-5 refers to the opaque line in row A and column 5. Row A consists of opaque lines on a clear background, and row B consists of clear lines on an opaque background. These opaque and clear lines are used for calibrating optical microscopes used to measure linewidths of isolated lines of either or both polarities. Row E consists of patterns with opaque line pairs (the two interior lines of shorter length)* for calibrating the length scale of optical microscopes by measuring the distance between line centers (pitch). Row F consists of patterns with two adjacent lines and the intervening space (two interior lines of longer length and the intervening space)* with approximately equal line and space widths. These patterns are used in setting the line-to-space ratio (contrast, threshold level, or linearity) on video image-scanning instruments. The widths of the left interior line and central space are certified. Row G consists of two patterns, with a series of 10 approximately equally spaced opaque lines in each pattern, to be used as a linear scale in checking for errors in the linewidth measurement system (e.g., the magnification as a function of position over the field of view). The center-to-center distances from the first line to each of the other nine lines of these patterns are certified. All rows on this SRM contain a broken horizontal fiducial line which is used to define the measurement position of each pattern.

3. Calibration of SRM 475

3.1 The Measurement System

All measurements of the SRM feature dimensions were performed at NIST in a laboratory with temperature controlled at 21 °C (± 2°) on the optical linewidth measurement system diagrammed in figure 4 [1].

The carefully aligned optical transmission microscope is mounted on a vibration isolation table. The photomask is placed on a scanning piezoelectric flexure-pivot stage with finely controlled motion in the *X* (scanning) and *Z* (focus) directions; this stage is mounted on another stage with coarse motion leadscrews in the *X* and *Y* directions to allow positioning of the desired feature in the field of view.

---

*The two outer lines of each pattern in rows E and F serve as "guard lines" during the photolithographic etching process to equalize proximity effects along the line edges and are not calibrated.

The photomask is illuminated from below with Köhler illumination (i.e., each point on the lamp filament evenly illuminates the entire specimen) from an incandescent source filtered at 530 nm wavelength with a coherence parameter of 2/3 (.60 numerical aperture condenser lens and .90 numerical aperture objective lens). A 20 x 400 μm slit is fixed on axis in the image plane in front of a photomultiplier tube. Image magnification at the slit is 157 times, giving an effective measurement area on the photomask of 0.127 x 2.55 μm, which is centered top-to-bottom on the feature (at the fiducial line). The photomultiplier output is amplified and digitized by a 12-bit analog-to-digital converter (ADC). Stage motion in the scanning direction is measured by a laser interferometer with resolution of 125 points per micrometer. All these devices are connected via appropriate control hardware and IEEE-488 bus to a dedicated desktop digital computer.

3.2 SRM Calibration Procedure

An outline of the overall calibration procedure is charted in figure 5. Before each complete SRM calibration, selected features on a control photomask are measured and compared with control history to ensure that the system has not changed or drifted. These selected features include spacing patterns E-4, E-5, and G-1 which have been independently calibrated by the Dimensional Metrology Group at NIST [2] to provide traceability to the standard meter. Each feature on the SRM being calibrated is then measured in sequence and the sequence repeated nine times. After each SRM calibration is completed, the control photomask is measured again.

All measurements, including the control measurements, are entered into the linewidth database. After the calibration measurements are completed the database is searched to ensure that the control was measured before and after the calibration and that these two control measurements were statistically invariate. The database entries for the calibration are combined and examined statistically: the standard deviation for each feature is calculated, number of measurements checked, etc. Criteria must be met for each of these statistical factors. If necessary, more measurements can be made and added to the database.

Once all the above conditions are met, the certificate is printed and the SRM linewidth standard is released to the Standard Reference Materials Program Office for sale. All of the calibration database files for this serial number are then stored on one flexible disk along with summary data. The disk is kept for archival storage along with the printed calibration results for each measurement, a printed summary of the statistical data, and dark-field illumination micrographs of the calibrated pattern.

3.3 Specimen and Measurement Axis Alignment

The measurement axis is the axis of the interferometer laser beam (actually the geometric center of the four beams used in this interferometer) and is defined as the X-axis. The scanning axis is the axis of motion of the piezoelectric scanning stage, and the specimen axis is a line on the surface of the photomask perpendicular to the length of the linewidth feature being measured. Ideally these axes would coincide, but in practice it is not possible to locate these axes with great precision.

In this application the perpendicular distance between parallel lines (the right edge and left edge of a feature) is measured. It is important to align the specimen axis with the measurement axis, but slight misalignment of the scanning axis causes no error because only the component of motion parallel to the measurement axis is measured and this is also the component parallel to the specimen axis. In other words, a scanning axis misalignment will cause the width measurement to "slide" slightly along the length of the line, but it will always be parallel to the line's width. Even so the scanning axis is aligned as carefully as possible, first by aligning the leadscrew stage by moving it back and forth in the Y direction and adjusting its rotation in the X-Y plane until the interferometer indicates no periodic change in X, and then by geometrically aligning the piezoelectric stage by eye.

Misalignment of the specimen axis with the measurement axis will lead to a geometric error proportional to 1 - cos(*misalignment angle*). This alignment is checked by scanning and measuring the X position of the center of the long vertical fiducial line at the right side of the pattern (see fig. 3) near its top and bottom ends. The angle of rotation of the specimen can be calculated from the positions of these centers and the nominal distance between them. After the specimen has been mounted and aligned by eye, the alignment is checked and readjusted until the program indicates the specimen is properly aligned. The calibration program will not commence taking data unless the misalignment angle is less than $\pm$ 0.1°. This allows a maximum cosine error of 1.5 ppm, or .06 nm on the longest feature on this photomask. If the specimen is tilted (i.e., the specimen stage is rotated about the Y-axis), the leading and trailing edges of the longer patterns will not both be in focus, and this condition will be detected in the measurements.

A significant potential error source is the Abbé error caused by possible offset between the measurement axis and the specimen axis in combination with angular motion of the scanning stage. The Abbé offset in the linewidth measurement system is less than about 2 mm. Comparison of pitch measurements made on this apparatus and on the NIST Line Scale Interferometer (see sec. 3.6) allow compensation for errors of this type. Small random rotations of the scanning stage contribute to the measured random uncertainty.

3.4 Feature Measurement Sequence

A flow chart of the main steps of the feature measurement sequence is given in figure 6. The feature to be measured is first centered in the field of view, then focused and scanned as the optical profile position and intensity data are taken and stored as two one-dimensional arrays. The data are then low-pass filtered to reduce extraneous noise and processed to find the edge locations. Linewidth is then calculated.

Position and intensity data points are correlated by alternately triggering the interferometer and the voltmeter to take one reading each in a software loop while the scanning stage is moving. There may be a few clock cycles delay between the two readings of a data pair, but this delay is very small (corresponding to 2 nm/ms of delay) and is the same at leading and trailing edges; thus, it cancels in the linewidth or pitch calculation.

Image profiles such as those in figure 7 are presented on the computer screen during data acquisition and processing to allow monitoring system operation. After passing several data quality checks, the results are entered into a database for the SRM being calibrated.

A more detailed description of the measurement sequence and system can be found in reference [1].

3.5 Edge Location Determination

Analysis of optical microscope imaging gives the following equation for image intensity at the edge of a line [3]:

$$T_c = R_t\,(I_o + I_m + 2\sqrt{I_o\,I_m}\cos\phi), \tag{1}$$

where T_c is the intensity of the light at the threshold point (edge) on the image profile (see fig. 8); I_o is the intensity of the light passing through the not-perfectly-opaque chromium layer; I_m is the intensity of the light passing through the clear areas (beyond the diffraction peaks); and ϕ is the optical phase difference of the light transmitted through these two areas. R_t is a theoretically derived ratio, of approximately 0.25, which varies slightly depending on the coherence factor, viewing slit width, focus, proximity of the next edge, and other imaging conditions. For the conditions of measurement of this SRM in the NIST calibration system, R_t varies from 0.25 to 0.28 (see last paragraph of this section).

Real microscope images often include some flare light (light scattered off the microscope components illuminating the otherwise opaque features on the photomask from above or reaching the image plane by indirect paths). In nonlaser illumination systems, this light is temporally incoherent with respect to the light comprising the diffraction pattern (image profile) and simply adds incoherently (intensity-wise) to each intensity of the image profile.

To a first approximation the intensity of the flare light is not a function of position across a feature. Therefore, the effect of the flare light can be incorporated into eq (1) by simply subtracting its value from each intensity component on the image profile:

$$I_o = I_o' - I_f;\quad I_m = I_m' - I_f;\quad T_c = T_c' - I_f, \tag{2}$$

where the prime designates an observed intensity (including the effects of diffraction, transmission, and flare) and where I_f is the magnitude of the flare light component in the image profile for each feature. Substituting into eq (1) gives:

$$T_c' = R_t\,[(I_o' - I_f) + (I_m' - I_f) + 2\sqrt{(I_o' - I_f)\,(I_m' - I_f)}\cos\phi] + I_f. \tag{3}$$

Both ϕ and I_f must be known to evaluate the threshold condition. I_f is feature and background dependent and must be determined for each feature. For this SRM, where the antireflecting-chromium layer can be considered to be homogeneous, the transmittance (Tr) and ϕ can be taken as constants and I_o can be expressed as ($Tr \times I_m$). Then, considering that (I_m - I_o) equals ($I'_m - I'_o$) and substituting in eq (2), it can be shown that

$$I_f = [I'_o - (Tr \times I'_m)] / (1 - Tr). \quad (4)$$

The transmittance of the SRM was determined by using the linewidth measuring system to measure the intensity of light passing through the chromium near the center of the large chromium-covered upper-left quadrant of the mask and found to be about 0.18% of the incident intensity.

There is no known simple method for determining ϕ. However, a recent study of image profiles generated by a computer model [3], developed by D. Nyyssonen, of the NIST microscope system indicates that linewidth uncertainty from not knowing this phase difference is no greater than 15 nm if the threshold intensity used to determine the edge location is that for the case where ϕ equals $\pi/2$. This uncertainty is included in the systematic error budget. The model is based on the theory of partial coherence and allows variation of image formation conditions such as: linewidth, wavelength of incident radiation, transmittance and phase of the object and background illumination, and slit width. Profiles generated by this model agree very closely with profiles generated from the measurement data. Profiles were generated for lines and spaces 0.50 to 15 μm wide where the transmittance of the "opaque" areas is 0.2% and ϕ ranges from 0 to π. The results of the study also indicate that the relative threshold intensity varied from 25% to 28% of (I_m - I_o) over the range of widths simulated, (fig. 9). Therefore, an algorithm for determining linewidth was implemented that assumes a phase difference of $\pi/2$ and iteratively selects the threshold intensity ratio from this model-generated data according to the linewidth of the feature being measured.

3.6 Precision and Accuracy of the SRM Calibration

The SRM certificate reports the measured linewidths and pitches (spacings). The reported values are the average of at least nine repeated measurements. The certified linewidths and pitches have separate uncertainty values because of subtle differences in the way errors affect the measurement of widths and pitches. The uncertainty statement given is based on two contributing factors: precision and accuracy.

Process precision is defined as the variability observed in repeated measurements of a single physical quantity under essentially the same conditions [4] and is intended to describe the reproducibility of the measuring device, the optical microscope, as well as all of the environmental conditions which may affect the measurement [5]. A numerical value for process precision cannot be determined until the measuring system is operating in a state of statistical control and the source of variability is shown to be random in nature and stochastically stationary. When these criteria have been met the process standard deviation

quantifies this random error. The value for the process precision on the certificate of calibration includes the variability of the control measurements and the variability of the nine repeated SRM measurements. The details for computing this value are given in the Appendix.

Accuracy is the closeness of agreement between an observed value and the true value [6]. Pitch measurements of several features in a control SRM have been independently calibrated by the Dimensional Metrology Group on the NIST Line Scale Interferometer. Comparison of these measurements with measurements of the same features made on the NIST optical linewidth measurement system provides a scale correction factor to be applied to the SRM calibration measurements. Typically, the scale correction factor is equal or nearly equal to 1.0, indicating there is no significant scale difference between the two measurement systems. This comparison adds a small systematic uncertainty to all measurements (see appendix, sec. E).

The laser interferometer used to make these dimensional measurements is subject to a sinusoidal nonlinearity along the beam path due to polarization mixing. This leads to a maximum periodic systematic error of ~ 3.5 nm every one-quarter wavelength (0.16 μm) for the four beam differential interferometer used here [7]. Since repeat measurements of each photomask feature are made at substantial time intervals, thermal drift in the apparatus insures that these measurements are randomly distributed over this quarter-wavelength period. Thus this error is random, with deviations from the mean wavelength equally likely to be positive or negative, and is included in the calculation of process precision.

The index of refraction of air, and hence the interferometer wavelength, depends on its temperature, pressure, and composition (relative humidity, CO_2, etc). In this measurement system this can lead to error in two ways: the index error times the interferometer deadpath changes the apparent position in the measurement of each edge, and the index error times the measured length changes the length scale.

The deadpath here (the minimum distance between the fixed and moving mirrors) is about 1 cm. The measurement of linewidth or pitch, however, is a differential measurement in that the difference of the positions of the leading and trailing edges is measured by measuring the positions of both edges within a very short time (19 s for the longest pattern on this SRM); the line's width is being measured, not its position. A deadpath error can occur then only if the index of refraction changes in this time interval. Since such changes (caused, for instance, by convective turbulence) are equally likely to be positive as negative, this type of error is random and is included in the measured precision. The maximum magnitude of this deadpath error is 30 nm/°C/min, but since the temperature must decrease after it increases, this error is random and not systematic.

If the temperature is constant but not at the nominal value (20 °C) there will be an index of refraction error of approximately 1 ppm/°C. The worst case error for a 3 °C temperature offset is then 0.11 nm. An atmospheric pressure deviation of 30 mm Hg from the nominal 760 mm Hg changes the index of refraction by 9 ppm, leading to a 0.34 nm error on the longest feature. Deviation from nominal of the other factors listed above results in similar but much smaller random errors.

In the field of optical submicrometer linewidth metrology, the ideal reference standard with features which have vertical walls and smooth edges does not exist. Instead, real features have erratically varying, nonvertical edge geometries and raggedness along their length [8] (see fig. 10). The effective length of the viewing slit in the NIST instrument is 2.6 μm, and the linewidth reported is the average over this length, positioned at the center of the line. Therefore, both the nonvertical edge geometry and the raggedness along the length of the line are estimated as averages along the edge of the line. To quantify these systematic uncertainties the feature edge geometry is examined with a scanning electron microscope. As this examination precludes use of the photomask as an SRM, only one sample from each photomask production batch is examined.

Typically, the SEM micrographs of the photomask features show that the raggedness along the length of a line is less than 30 nm and has a spatial period of 100 nm or less. If the user's measurements of this SRM are also averaged over a length comparable to that of the NIST viewing slit, uncertainties due to edge raggedness become insignificant.

A determination of the uncertainty caused by the nonvertical edge geometry is accomplished by estimating the difference between the edge location at the top surface and the corresponding edge location at the substrate level, as illustrated in figure 11. Estimates are made at uniform intervals along a 1 μm section of the sample as imaged in an oblique view SEM micrograph. The uncertainty is determined as the average of these estimated edge location differences. For width measurements, edge location errors for the right and left edges tend to add; thus the linewidth uncertainty is twice the edge location uncertainty[9].

The linewidth uncertainty value given on the certificate data sheet for rows A, B, and F includes the uncertainty resulting from the nonideal edge geometry estimated from the SEM micrographs (typically around $\pm$30 nm), $\pm$15 nm introduced by assuming a phase difference of $\pi/2$ radians (see sec. 3.4); and $\pm$5 nm of less quantitatively defined systematic errors.

Because pitch measurements involve measuring the distance from one location (left edge, right edge, or center) on one feature to the same location on another feature, edge detection errors tend to cancel and are not included in the uncertainty reported for row E and row G measurements.

The measurement precision is determined for each SRM photomask as described in the Appendix and the pooled 95% confidence levels are reported for the width (rows A, B, and F) and pitch (rows E and G) measurements on the certificate data sheet.

The uncertainty of the width and pitch values reported is a combination of the appropriate systematic uncertainties and measurement precision. A summary of the error components is given in table 1.

The user is advised to examine the edge properties of the production photomasks to be measured. If the quality of the edges of the features on the user's photomasks is significantly inferior to that of this SRM, an additional level of uncertainty should be added to the uncertainty of measurements made on the user's photomasks.

4. Using SRM 475

The following section provides information on the care and handling of the SRM photomask and gives basic instructions and precautions on its use for calibrating optical microscope systems for measuring linewidths of features on antireflecting photomasks or similar artifacts.

4.1 Special Precautions

Contamination or damage can change the measured linewidths, invalidating the NIST calibration. Particular care should be taken during use to avoid bringing the microscope objective, or any other object, into contact with the top (chromium-coated) surface of the SRM. It is recommended that users calibrate secondary standards of their own design and use these in routine calibrations while keeping the NIST standard in safe storage. If this is done, the secondary standards should be checked periodically against the NIST standard. Also, it may be advisable for the user to calibrate one or more of the uncalibrated patterns on the SRM for use in the event that the NIST calibrated pattern is destroyed.

Precautions should be taken to prevent the accumulation of airborne and other contaminants on the SRM. If cleaning becomes necessary, use only noncorrosive wetting solutions (surfactants) at room temperature.

For cleaning we recommend the following procedure:

Soak the SRM for 15 minutes to several hours in a mild solution of commercial mask cleaner and de-ionized water.
While the mask is still immersed, brush the coated side gently with a soft lens brush - stroke parallel to the calibrated line length and in one direction.
Rinse the mask thoroughly with de-ionized water.
Blow away water droplets with a stream of clean, dry air or nitrogen at room temperature.

If the contamination persists, apply a few drops of undiluted mask cleaner directly on the SRM before repeating the above cleaning process.

Removing fingerprints or other greasy contamination may require rinsing the SRM with alcohol or acetone and repeating the above cleaning process.

Inappropriate use of the NIST linewidth standards can result in inaccurate calibrations and may invalidate traceability to NIST. The practices most apt to give inaccurate calibrations when using the NIST linewidth standard include:

a. Using the linewidth standard to calibrate a measurement system that will then be used to measure linewidths on specimens with optical properties that differ significantly from those of the standard (for example, features on silicon wafers). One important requirement for accuracy is that the image profile (or diffraction pattern) of the edge have the same shape for both the standard and the user's specimens. These image profiles will not have the same shape if the optical properties of the standard and the user's specimens differ.

   When calibrating optical measuring systems that use transmitted light it is especially important that the transmittance of the standard and the user's specimen match at the measuring wavelength. The transmittance of SRM 475 is less than 0.2% at a wavelength of 0.53 μm. Line edge location conditions for photomasks with transmittance greater than about 0.5% may be significantly different from those of the SRM.

   When calibrating optical measuring systems that use reflected light, the standard and the user's specimen should match even more closely. The more important properties to match are the complex reflection coefficient of the patterned metal layer and the substrate, the thickness of the patterned layer, and the transmittance of the patterned layer.

b. Using the linewidth standard to calibrate a scanning electron microscope. This SRM is designed specifically for use with optical microscopes and, as no criterion has been established for edge location in an SEM image, this SRM cannot be used to calibrate an SEM for linewidth measurements. Its use in an SEM is further discouraged because the profile of the feature could change as a result of coating the SRM with an evaporated film to reduce electrical charging, of deposition of contamination during operation of the SEM, and of detachment of the chromium during cleaning to remove evaporated films or contaminants. (The substrate of this SRM is quartz and, even when low-voltage SEM techniques are used it is next to impossible to view the SRM features in the SEM without first coating the sample).

c. Failing to correct for scattered (or flare) light. Although the chromium pattern on SRM 475 is not highly reflective, it includes isolated features surrounded by various large clear areas and the image profiles may exhibit a moderate component of scattered light which may vary from feature to feature and from the user's specimen. The intensity of the scattered light should be subtracted from all measured intensity levels before determining the edge location. This correction has been made in the calibration of SRM 475. If the user cannot make this correction, the reflectance and transmittance of the standard used for calibration should match the reflectance and transmittance of the user's specimen at the measuring wavelength. At the present time, NIST has a companion bright-chromium linewidth standard (SRM 476) that has the same pattern as SRM 475. We recommend that the user: (1) use the SRM that most closely matches the specimens to be mesured and (2) make the scattered light correction outlined in step 7.

d. Using the NIST linewidth standards to generate a calibration curve that is then used for features that are larger than the largest or smaller than the smallest feature on the standard. The nominal linewidth range of SRM 475 is from 0.9 to 10.8 μm and this SRM will not adequately calibrate a microscope outside of this range. This is especially true for extensions much below the nominal range where the calibration curve becomes nonlinear. NIST is developing another antireflecting-chromium linewidth standard, SRM 473, that will extend the linewidth range down to 0.5 μm and up to 30 μm.

The user should be aware that all standards have a precision and accuracy of calibration associated with them and, to this extent, are not perfect. The calibration of a microscope using a standard has an imprecision associated with that calibration and also has an imprecision associated with the subsequent use of that calibrated microscope to measure an unknown specimen. Therefore, the accuracy of the user's measurements cannot exceed the accuracy of the standard. The uncertainty of the final measurement on the unknown specimen is a combination of the accuracy of the standard used for calibration, the precision of the calibration measurements using the standard, and the precision of the measurements of the unknown specimen.

These and other topics are discussed more fully in the references [1, 14]. The need to use good measurement techniques to achieve the best results with these linewidth standards cannot be overemphasized. The user who knows more about the potential problems is more likely to make better use of the linewidth standard.

4.2 Microscope Calibration Procedures

The following procedure is recommended for using this SRM to calibrate optical microscope systems for measuring linewidths on antireflecting photomasks. It is assumed the user is familiar with the operation of the microscope system being calibrated, and no attempt is made to give detailed instruction on the use of microscope systems; however, instructions on setting up an optical microscope with Köhler illumination for dimensional measurements can be found in reference [10].

Procedures	Explanatory Notes
1. Set up the measurement system for dimensional measurements using the same procedures that will be used for measuring photomasks.	Follow manufacturers instructions or consult reference [10] for recommended procedures including adjustments for Köhler illumination.
2. Locate within the microscope field-of-view the specific pattern group on the SRM that has been calibrated by NIST.	Each pattern group has a pattern number located to the left of row E. The SRM Certificate identifies the calibrated pattern group (see fig. 2).

Procedures - continued

3. Check the resolving power of the microscope objective by focusing on feature G-0. If the objective cannot clearly resolve the 10 lines, use another objective.

4. Align the SRM so that lines are measured in a direction perpendicular to their length.

5. Adjust the measurement system length scale to give the same reading for the spacing of the two inner lines of feature E-5 (see fig. 3) as the NIST value.

6. Check for mechanical nonlinearity and/ or optical distortion by measuring the spacings of the 10 lines in feature G-0 (or G-1) and comparing the results with the NIST values.

   For all further measurements, use only the portion of the field of view corresponding to the location where the differences from NIST values are relatively constant or that portion of the video-display which exhibits minimum distortion.

7. Adjust the line-to-space ratio by measuring the calibrated line and space of a feature in row F.

   Subtract out the flare light (I_f) for each measurement by shifting the intensity zero level so that $I'_o = 0$ (see fig. 8).

Explanatory Notes - continued

The features within each pattern group are located by reference to an alpha-numeric grid with the letters A, B, E, F, and G identifying the row and the numbers 0 through 9 identifying the column (see fig. 3).

The long vertical line, running from row A to row G at the far right (see fig. 3) may be used as an alignment aid.

Do <u>not</u> use any other standards or procedures for this adjustment of the length scale unless specifically instructed otherwise by the manufacturer of the instrument.

To differentiate between optical and mechanical errors, multiple tests must be made. For example, repeat the test with interchanged optics while using the same screw thread to determine if a given error pattern is due to mechanical errors rather than optical distortion. If the errors are small, restricting the field of view may eliminate the necessity of identifying the error source.

The widths of the left inner (long) line and the adjacent space between the two inner lines are certified.

Determination of I_f for each feature by using eq (4) (sec. 3.5) would be time consuming and impractical for the user; however, because the transmittance of this SRM is less than 0.2%, I'_o and I_f are nearly identical and the user may consider all measured I'_o intensity to be flare light.

Procedures - continued

Explanatory Notes - continued

Adjust system contrast, brightness (on video-type image-scanning micrometer attachments) and/or threshold until both (line and space) measured widths agree as closely as possible with the NIST values.

Accurate linewidth measurements require a fixed relationship between a threshold in the image intensity profile, which corresponds to the physical line-edge location, and the video output or other signal from which the measurement is obtained.

Determine the ratio T_c'/I_m' and use this ratio to set the threshold level for each subsequent measurement in this calibration session.

NOTE: If any changes other than refocusing, repositioning and adjusting for flare are inadvertently made during the following steps, discard the data and start again with step 5.

8. Measure and record the widths of the calibrated features in rows A and B.

Use the same focusing criteria throughout.

For optical systems with Köhler illumination, a fine bright band (or other diffraction effects) may appear along the edge of the line image at best focus.

Do not refocus between setting on the left and right edges of the same line.

Make all measurements in the same direction of travel.

Some mechanical systems exhibit backlash when their direction of travel is changed.

Subtract out the flare light as in step 7.

A flare-light correction should be made when measuring linewidths on all photomasks (not only this standard).

9. Measure and record the line spacings (pitch) of NIST calibrated line pairs in row E.

10. Derive the calibration curves as described in reference [11].

These calibration curves apply only to this system/operator combination.

The system is now ready for measurement of other antireflecting-chromium photomasks or artifacts with similar optical properties to SRM 475 (low reflectance and very low transmittance) using the same threshold value and flare-light correction procedure. If the

user attempts to measure artifacts with chromium layers having transmission much greater than 0.2%, it may be necessary to measure the phase angle, ϕ, and use eq (3) to determine a different edge location threshold. These procedures are beyond the scope of this report.

Repeat the complete calibration procedure on a routine periodic basis and whenever a substantial change is made in the measurement system. The time between periodic calibrations may have to be determined empirically.

ACKNOWLEDGMENTS

Parts of this document (especially the procedures in sec. 4) are based on the earlier SRM 474 and SRM 475 Handbook prepared by Diana Nyyssonen and John Jerke.

The photomicrographs used to examine the edge geometry were provided by the Scanning Electron Microscope Section (Sam Jones, William Keery, and Michael Postek) of the Microelectronics Dimensional Metrology Group.

Many thanks to Robert Larrabee for his guidance and advice and to Beverly Wright for typing the numerous revisions of this document.

REFERENCES

[1] Potzick, J., "Automated Calibration of Optical Photomask Linewidth Standards at the National Institute of Standards and Technology," SPIE Vol. 1087, Integrated Circuit Metrology, Inspection, and Process Control, San Jose, CA, February 1989.

[2] Beers, J., "Length Scale Measurement Procedures at the National Bureau of Standards", Natl. Bur. Stand. (U.S), NBSIR 87-3625, 1987.

[3] Nyyssonen, D., "Linewidth Measurement with an Optical Microscope: The Effect of Operating Conditions on the Image Profile," Applied Optics Vol. 16, August 1977, pp. 2223-2230.

[4] Ku, H.H., "Statistical Concepts in Metrology - With a Postscript on Statistical Graphics," Natl. Bur. Stand. (U.S.) Spec. Publ. 747, August 1988, pp. 12.

[5] Croarkin, C., "Measurement Assurance Programs Part II: Development and Implementation," Natl. Bur. Stand. (U.S.) Spec. Publ. 676-II, 1985, pp. 23.

[6] 1986 Annual Book of ASTM Standards, "Statistical Terminology for Statistical Methods," Designation E 456-83a, American Society for Testing and Materials, 1916 Race Street, Philadelphia, PA 19103.

[7] "High Performance Motion Control for Precision Equipment," Hewlett Packard, 1990, p. 34.

[8] Nyyssonen, D. and Larrabee, R.D., "Submicrometer Linewidth Metrology in the Optical Microscope," J. Res. Natl. Bur. Stand. (U.S.), May-June 1987, pp. 189-190.

[9] Potzick, J., "Practical Photomask Linewidth Measurements," SPIE Vol. 1261-13, Integrated Circuit Metrology, Inspection, and Process Control, San Jose, CA, 1990.

[10] Annual Book of ASTM Standards, Part 43, "Standard Practice for Preparing an Optical Microscope for Dimensional Measurements," Designation F 728-81, American Society for Testing and Materials, 1916 Race Street, Philadelphia, PA 19103.

[11] Croarkin, C. and Varner, R.N., "Measurement Assurance for Dimensional Measurements on Integrated Circuit Photomasks," Natl. Bur. Stand. (U.S) Tech. Note 1164, August 1982.

[12] Bullis, W.M. and Nyyssonen, D., "Optical Linewidth Measurements on Photomasks and Wafers," Chapter 7 in VLSI Electronics: Microstructure Science, Semiconductor Microlithography, Vol. 3, N.G. Einspurch, Editor, pp. 119-126 (Academic Press, New York, NY, 1982).

[13] Nyyssonen, D., "Linewidth Calibration for Bright-Chromium Photomask," NBSIR 86-3357, Natl. Bur. Stand. (U.S.), May 1986.

[14] Jerke, J.M., Croarkin, M.C., and Varner, R.N., "Interlaboratory Study on Linewidth Measurement for Antireflective Chromium Photomasks," Natl. Bur. Stand. (U.S.) Spec. Pub. 400-74, 1982.

Table 1. A listing of error sources and their contributions to overall measurement uncertainty. Errors are determined in a worst-case sense; scale factor uncertainties (in ppm) are multiplied by the largest dimension measured, giving scale errors of 0.03 nm (systematic) and 0.14 nm (random) for the largest linewidth (10.8 μm) and 0.11 nm (systematic) and 0.48 nm (random) for the largest pitch (36 μm). Net random error is derived from the measurements.

SUMMARY OF ERROR COMPONENTS

Systematic	Linewidth	Pitch
Laser wavelength accuracy	0.1 ppm	0.1 ppm
Axis alignment	3.0 ppm	3.0 ppm
Abbé error[1]	0.0 ppm	0.0 ppm
Substrate thermal expansion[1]	0.0 ppm	0.0 ppm
Refractive index of air[1]	0.0 ppm	0.0 ppm
Chrome edge geometry	50 nm[2]	0.0 nm
Chrome transmission magnitude & phase	15 nm[2]	0.0 nm
Comparison to Standard Meter	2.0 nm	3.0 nm
Other errors	3 nm	0.0 nm
TYPICAL SYSTEMATIC UNCERTAINTY	70 nm[2] TOTAL	3.1 nm TOTAL
Random		
Substrate thermal expansion	1.2 ppm	1.2 ppm
Refractive index of air	12 ppm	12 ppm
Deadpath refractive index	6.0 nm	6.0 nm
Polarization mixing	3.5 nm	3.5 nm
Vibration and noise	unknown	unknown
TYPICAL RANDOM UNCERTAINTY[3] (from measurements)	17 nm TOTAL	15 nm TOTAL

[1]These scale factor errors are removed by comparing the linewidth calibration system with the NIST Linescale Interferometer, which measures pitch only, giving traceability to the standard meter (see sec. 3.3, p. 4).
[2]Typical: depends on photomask batch.
[3]One standard deviation for a single measurement. Long-term [6 months, frequent mounting and dismounting] and short-term standard deviations do not differ significantly.

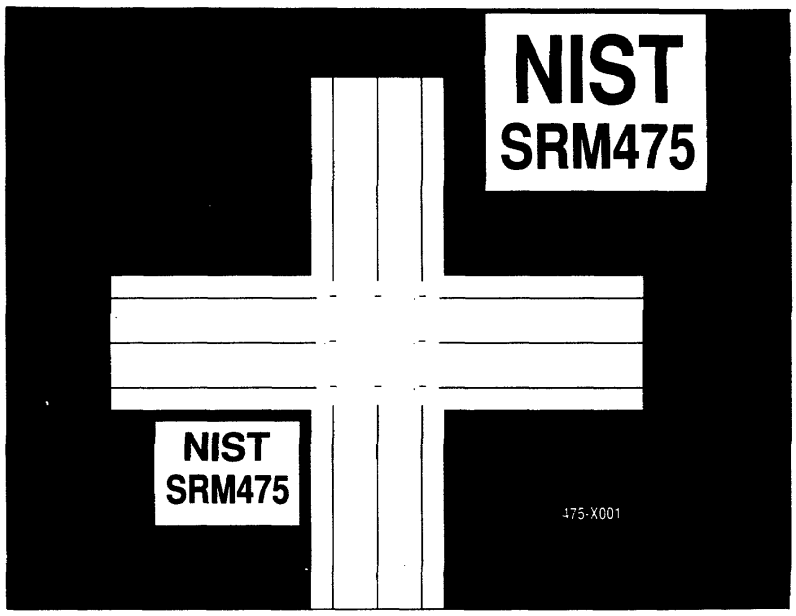

Figure 1. A view of the overall pattern on SRM 475. The basic measurement pattern is repeated eight times about the center. The horizontal and vertical lines help locate the patterns.

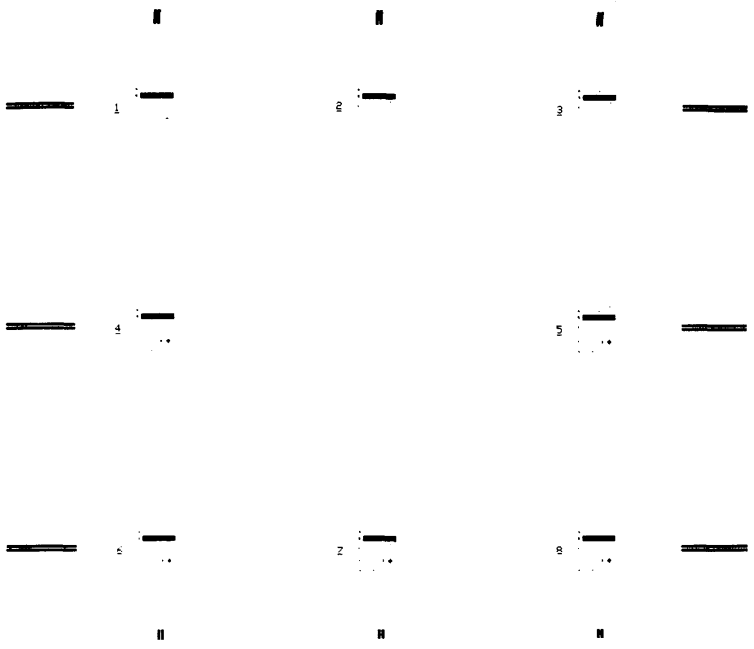

Figure 2. A view of the center of the SRM. The pattern number given with the serial number on the calibration sheet identifies which pattern has been measured by NIST. Pattern identification numbers can be seen to the left of each basic measurement pattern.

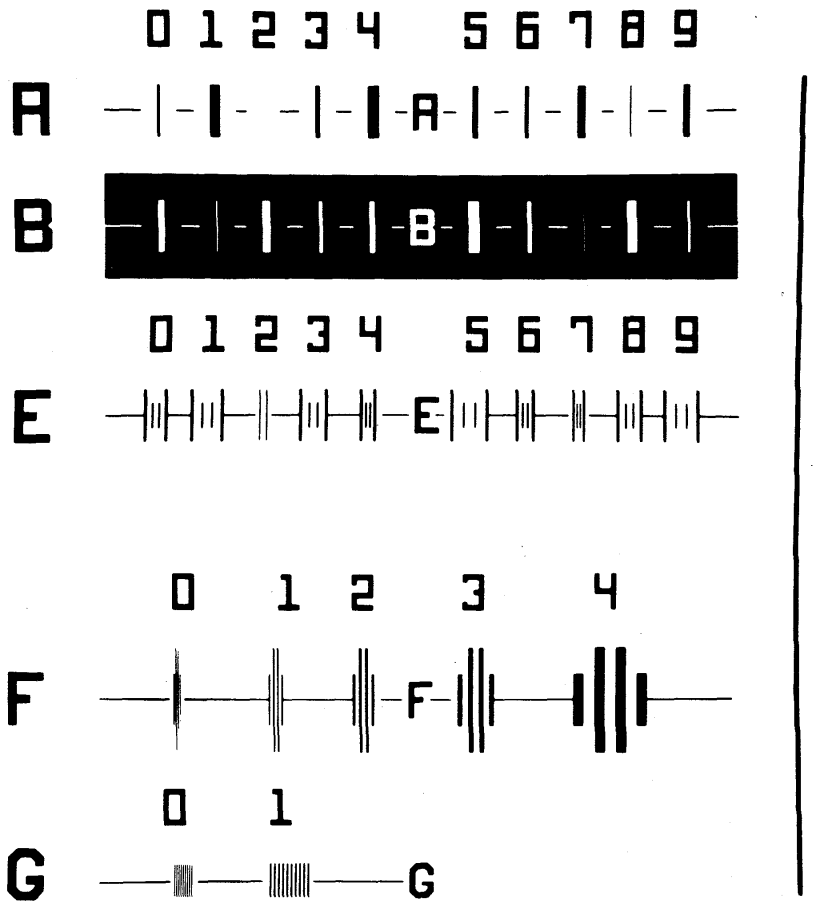

Figure 3. A view of one basic measurement pattern on the SRM. The individual lines and line patterns are located by reference to an alphanumeric grid with the letters identifying the row and the numbers identifying the columns. The long vertical line on the right is used to align the pattern on the measurement system. The broken horizontal lines mark the central calibrated area of the features.

Calibration values are given for: widths of opaque lines in row A and clear lines in row B; center-to-center spacing of the two inner (short) lines of each line pattern in row E; widths of the left inner (long) line and the space to its right of each line pattern in row F; and center-to-center spacings of lines relative to the first line on the left of each line pattern in row G.

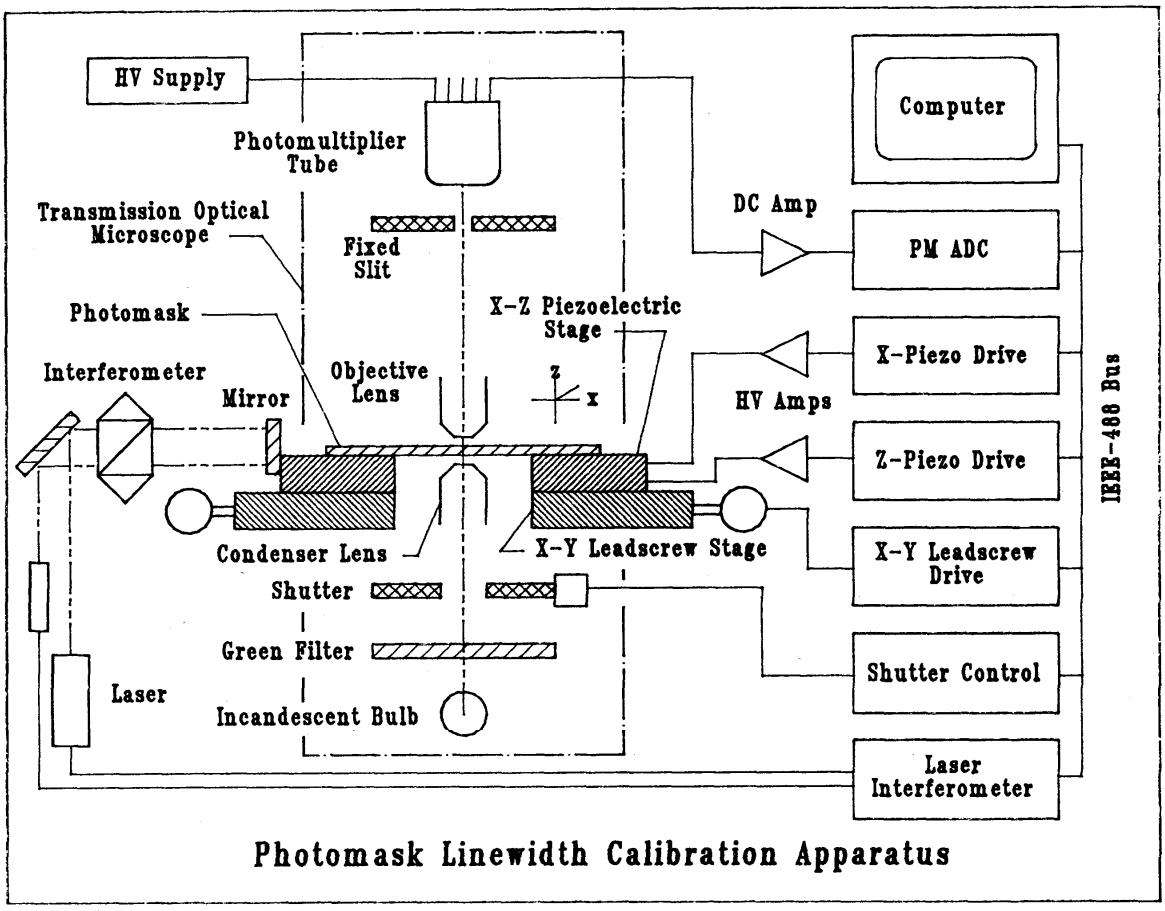

Figure 4. Schematic of the NIST automated optical linewidth calibration system. The photomask is placed on the scanning piezoelectric stage and is illuminated from below with partially coherent light from a filtered incandescent source. The measuring slit remains fixed while the image of the feature being measured is scanned past the slit by moving the photomask. The motion is measured with a laser interferometer and the image intensity at the slit is monitored with a photomultiplier. The digitized and amplified output of the photomultiplier and the interferometer output are connected via the IEEE-488 bus to the computer.

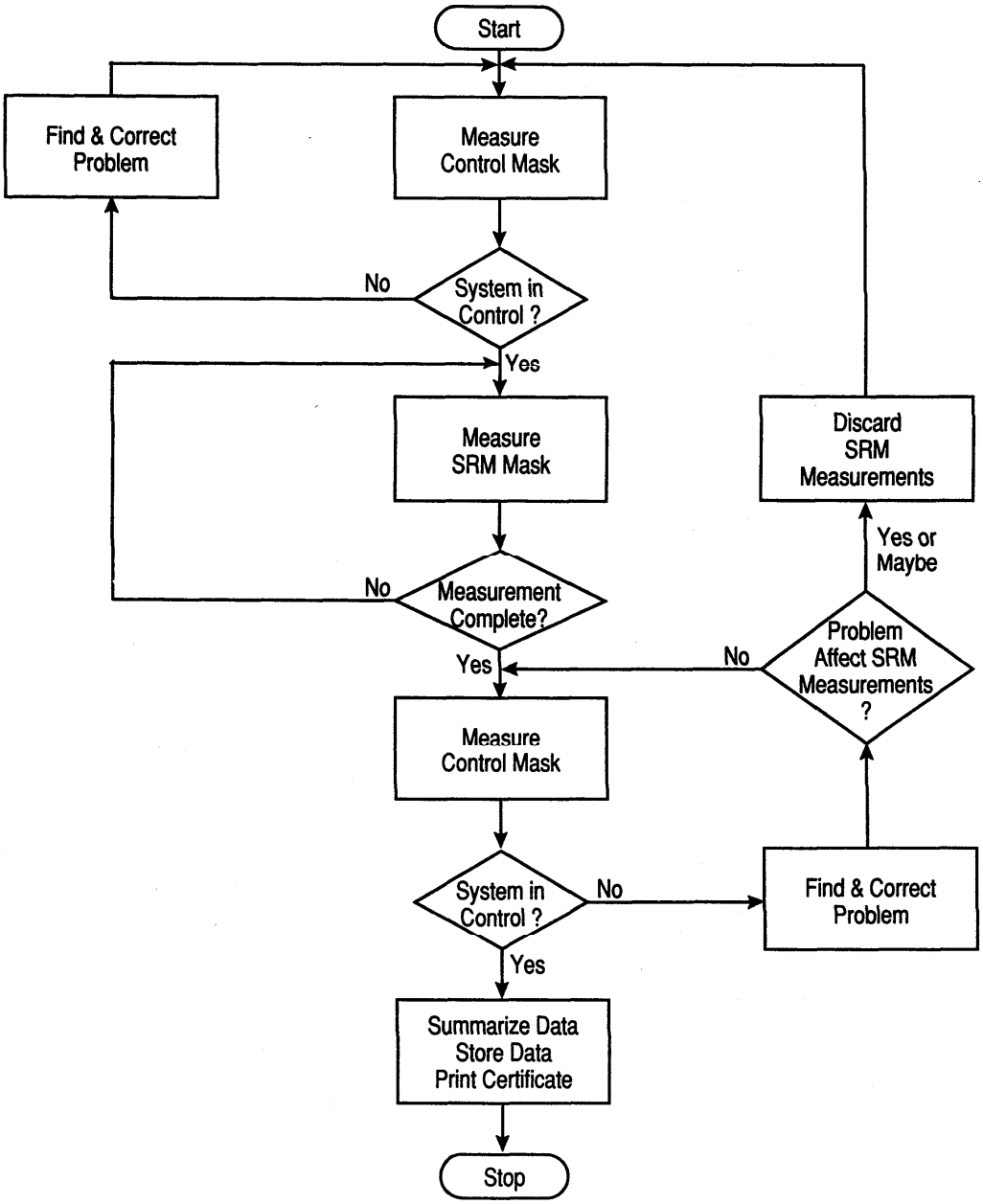

Figure 5. Flow chart outline of the overall calibration procedure for the calibration of SRM photomasks with the NIST optical linewidth measurement system. First, measurements are made on a control photomask and tested statistically to determine if the system is operating properly. Then, the SRM photomask is calibrated and the system operation is checked again by measuring the control photomask. If all tests indicate the system is within statistical control, a calibration certificate can be printed for the SRM photomask.

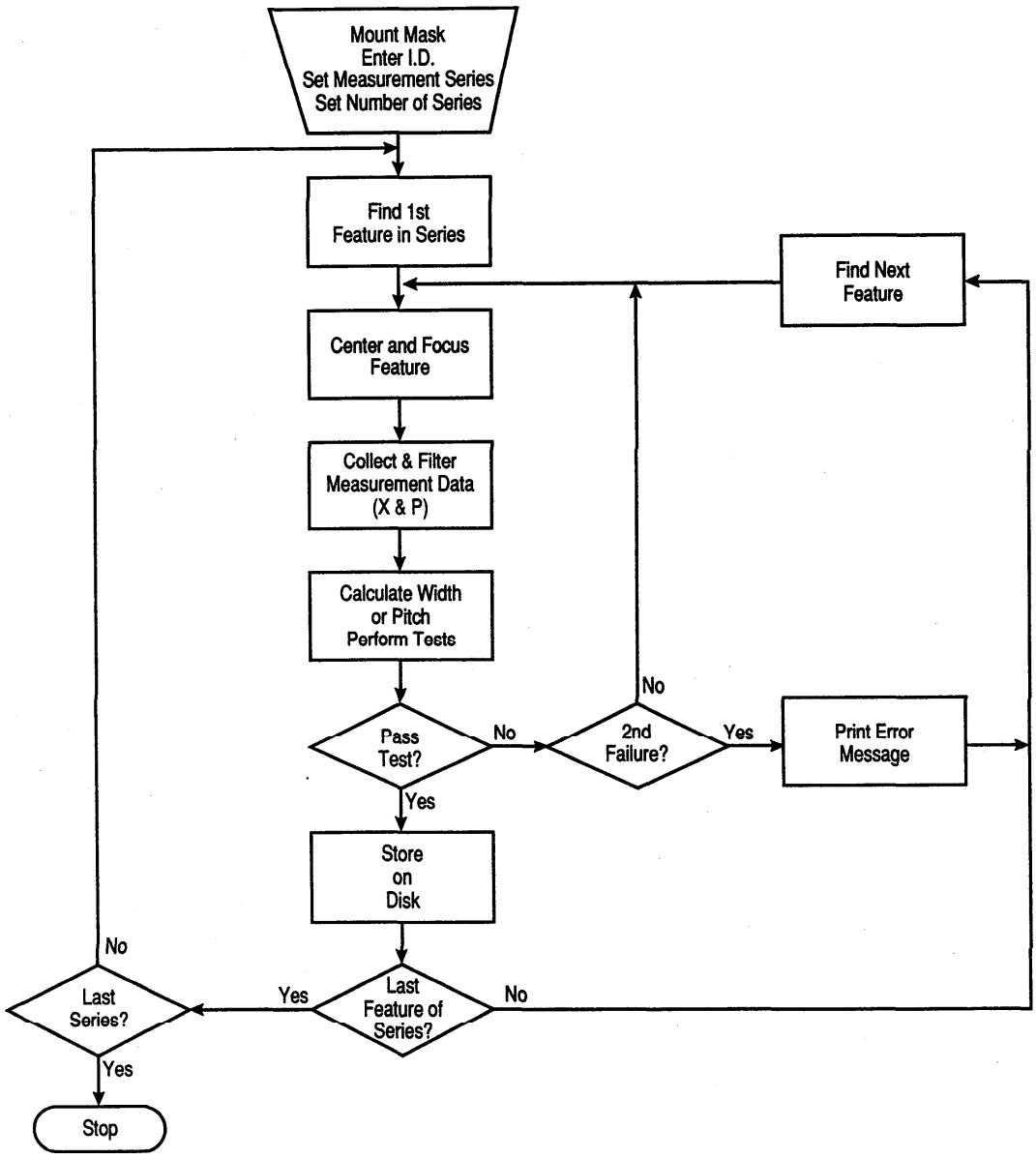

Figure 6. Flow chart of the main steps of the measurement sequence performed by the NIST optical linewidth measurement system. Each feature on the SRM photomask is centered in the microscope field of view, focused, and measured in sequence. The sequence is repeated until each feature has been measured nine times. The optical profile position (X) and intensity (P) are measured and the data are stored as two one-dimensional arrays.

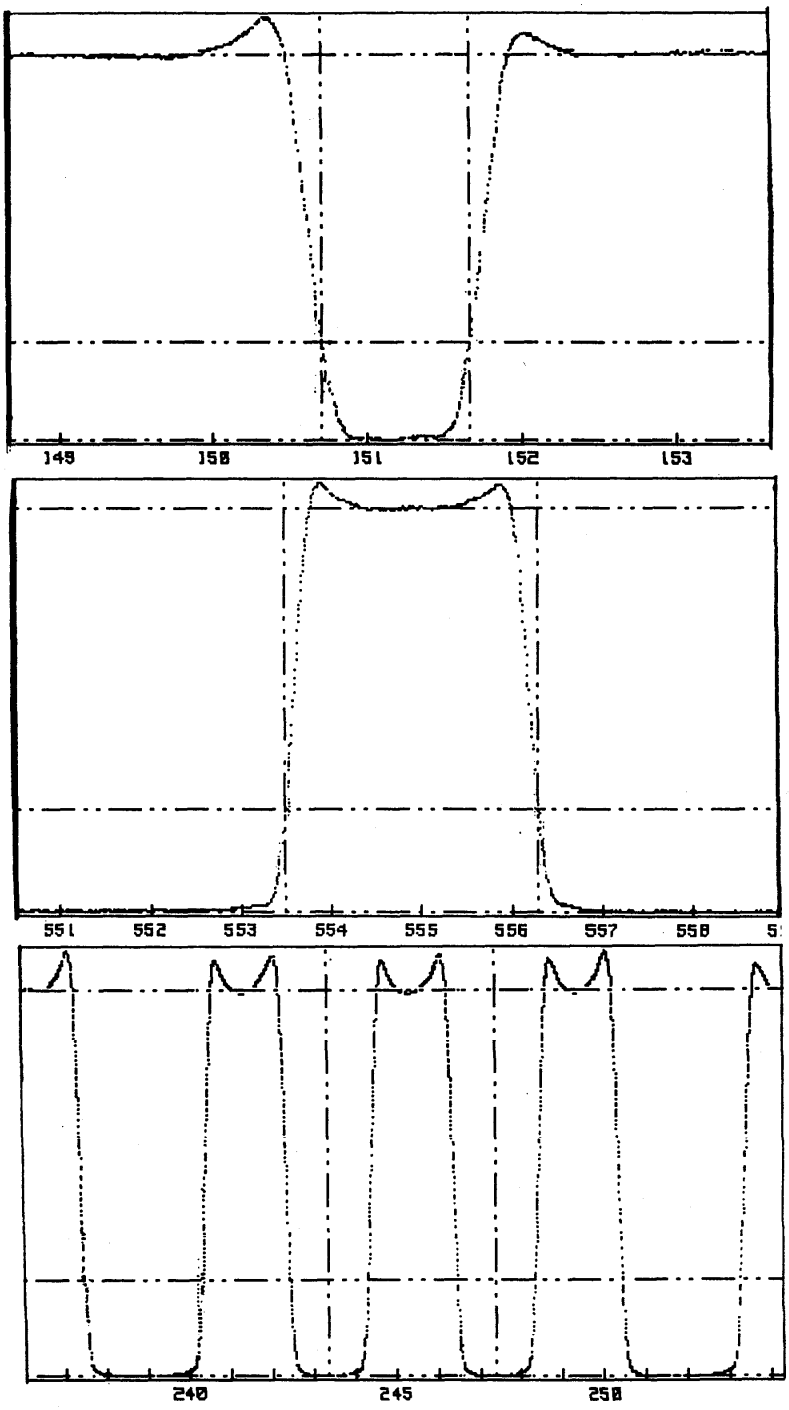

A. Profile typical of an opaque line in row A. The vertical fiducials mark the positions of the line edges.

B. Profile typical of a clear line (space) in row B. The vertical fiducials mark the positions of the space edges.

C. Profile typical of a line pair in row E. The vertical fiducials mark the positions of the line centers. The profile includes the two outer guard lines as well as the line-spacing pair.

Figure 7. Samples of optical profiles (measured light intensity versus position) displayed on the computer screen during the calibration process. The vertical axes are relative light intensity and the horizontal axes are position in μm. The horizontal lines are fiducials marking the relative intensity levels of the clear and coated areas and the threshold.

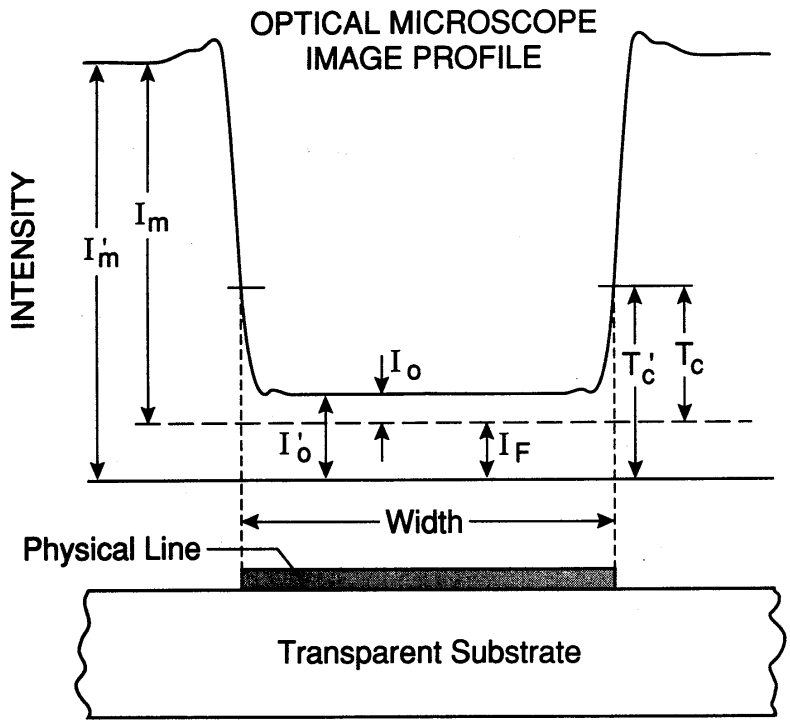

Figure 8. Schematic of the cross section of a vertical -edged chromium line and the corresponding optical profile of its microscope image. I_m is the intensity of the light passing through the clear area; I_o is the intensity of the light passing through the chromium; T_c is the intensity at the physical edge (threshold); I_f is the intensity of the flare light. The prime designates an observed intensity. The vertical axis is optical intensity and the horizontal axis is distance.

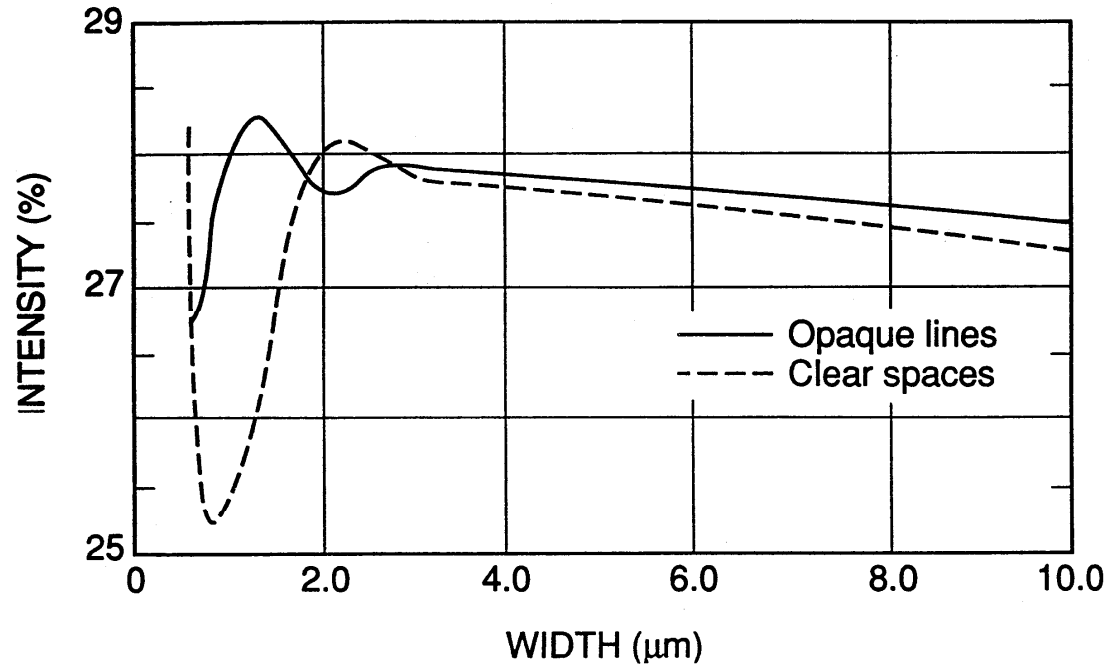

Figure 9. Optical intensity [% of (I_m-I_o)] at edge location versus linewidth, from a computer model of the NIST calibration system. Transmittance equals 0.2% and ϕ equals $\pi/2$ radians.

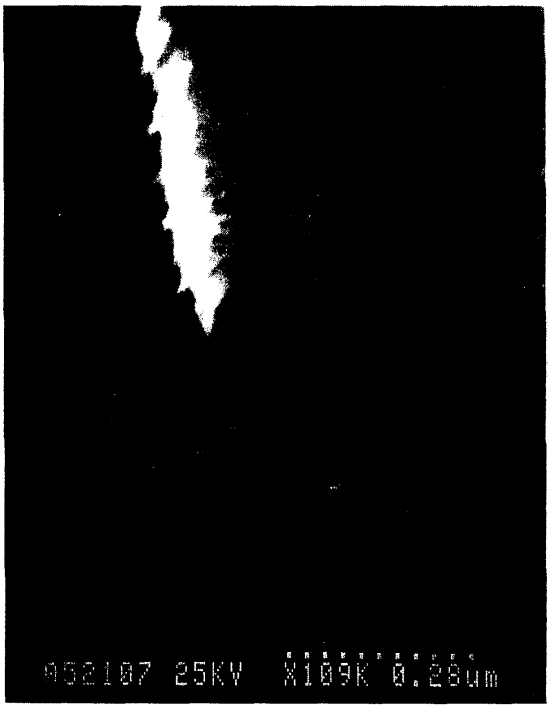

Micrograph A

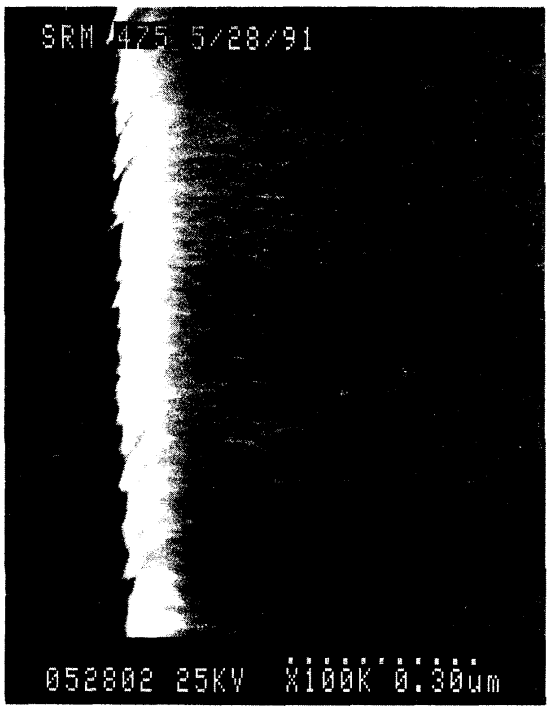

Micrograph B

Figure 10. SEM micrographs showing the nonideal nature of line edges on an antireflecting-chromium photomask. The scale is indicated by the row of eleven dots in the lower right of each micrograph. The dots are 28 nm apart in micrograph A, and 30 nm apart in B. Beam energy was 25 keV. The specimen in A is coated with gold; the specimen in B is coated with carbon.

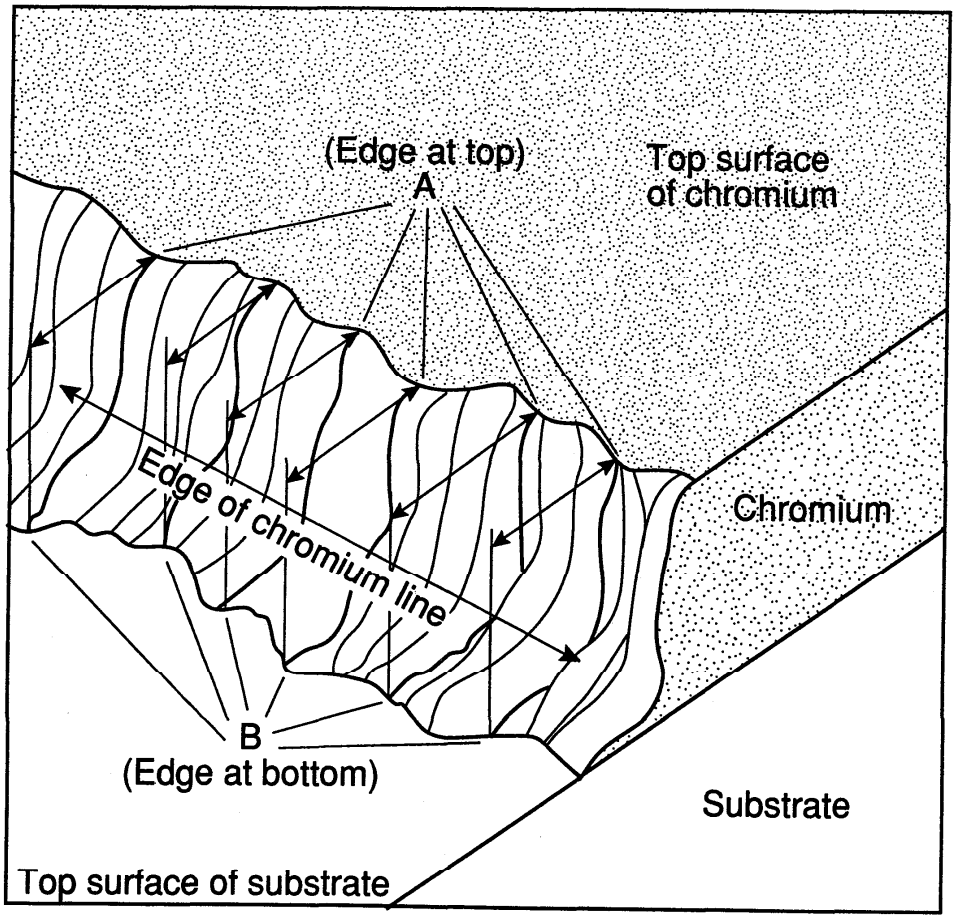

Figure 11. Schematic representation (not to scale) of a line edge as seen in an oblique view SEM micrograph. The uncertainty of linewidth measurements includes the uncertainty of the edge location resulting from non-vertical physical edge profiles. Determination of this uncertainty is accomplished by estimating the difference between the edge location at the top surface (A) and at the substrate level (B). Estimates are made at uniform intervals along a section of a specimen image in an SEM micrograph. The edge uncertainty reported is the average of such estimates made by several individuals using several different micrographs.

Appendix
Process Control for SRM 475 Calibrations

A. Introduction

The procedures used to assure statistical control of the linewidth SRM measurement system are defined. A control photomask with the same characteristics as the SRM photomask is used for measurement process control. Six of the features on the control photomask are measured each time an SRM photomask is calibrated. The six features are: the nominal 2.7 and 9.5 μm lines from row A; the nominal 9.5 and 2.7 μm lines from row B; and the nominal 4.0 and 10.8 μm pitch patterns from row E. These correspond to features A-0, A-1, B-8, B-9, E-4, and E-5 as shown on the diagram of a pattern in figure 12.

The purpose of the control photomask measurements is to provide a database that can be used to determine whether or not the measurement system is in a state of statistical control. There are several factors which may cause the optical measurement system to be out-of-control. There may be a change in the measurement system or a change in environmental conditions. This document describes the initialization of the database of control measurements, use of the database to determine if the measurement system is in control, and the maintenance of the database over a long period of time.

B. Initialization of Process Parameters

When the measurement system is determined to be ready for performing SRM calibrations, a database is initialized. This database consists of at least 15 sets of repeated measurements of the six selected features on the control photomask taken over a period of several weeks [15]. This period is representative of the normal operating mode of the optical measurement system. The six features measured are identified as A-0, A-1, B-8, B-9, E-4, and E-5. These features cover the extremes of the feature sizes and the range of the feature locations on the photomask. The database includes not only the measured width or space but also other pertinent information such as the date and time of the measurement and feature identification and any other potentially useful information (temperature, scan rate, etc.).

A plot, measured width or pitch versus time, of the repeated measurements for each feature is made to detect any possible anomalies in the measurement system and to verify that the system produces stable measurements whose variability is random in nature. The control database is accepted as being representative of the normal operating environment of the measurement system if no more than 5% of the measurements are suspected outliers (unexplained anomalies). If this is not the case, an effort is made to determine the cause and pertinent adjustments are made to the measurement system. The control database is then reinitialized.

The initial control database is used to estimate the mean vector (accepted mean values for each control feature) and the matrix of covariances between them. These are required elements for the multivariate Hotelling's T^2 test statistic [16]. The details for computing the estimate of the mean vector and the matrix of covariances are given below. The use of this test statistic and updating procedure for this statistic are given in following sections of this document.

From the database of control measurements for features A-0, A-1, B-8, B-9, E-4, and E-5, a matrix **[X]** is constructed, as shown below, of the N initial repeated measurements on the control photomask. Each of the features has the same number of repeated measurements,

$$\boldsymbol{X}_{ij} = \begin{bmatrix} X_{A0,1} & X_{A0,2} & \cdots\cdots & X_{A0,N} \\ X_{A1,1} & X_{A1,2} & \cdots\cdots & X_{A1,N} \\ X_{B8,1} & X_{B8,2} & \cdots\cdots & X_{B8,N} \\ X_{B9,1} & X_{B9,2} & \cdots\cdots & X_{B9,N} \\ X_{E4,1} & X_{E4,2} & \cdots\cdots & X_{E4,N} \\ X_{E5,1} & X_{E5,2} & \cdots\cdots & X_{E5,N} \end{bmatrix} \quad \begin{array}{l} \text{where } i = 1,2,\ldots.6 \\ \text{and } j = 1,2,\ldots.N\ . \end{array} \tag{B.1}$$

The average is computed for each of the features based on the N repeated measurements,

$$\begin{aligned} \bar{X}_{A0} &= \sum_{j=1}^{N} \frac{X_{A0_j}}{N} & \bar{X}_{A1} &= \sum_{j=1}^{N} \frac{X_{A1_j}}{N} \\ \bar{X}_{B8} &= \sum_{j=1}^{N} \frac{X_{B8_j}}{N} & \bar{X}_{B9} &= \sum_{j=1}^{N} \frac{X_{B9_j}}{N} \\ \bar{X}_{E4} &= \sum_{j=1}^{N} \frac{X_{E4_j}}{N} & \bar{X}_{E5} &= \sum_{j=1}^{N} \frac{X_{E5_j}}{N}\ . \end{aligned} \tag{B.2}$$

These values are the elements of the vector of means as denoted below:

$$\boldsymbol{M} = \begin{bmatrix} \bar{X}_{A0} \\ \bar{X}_{A1} \\ \bar{X}_{B8} \\ \bar{X}_{B9} \\ \bar{X}_{E4} \\ \bar{X}_{E5} \end{bmatrix}, \tag{B.3}$$

A matrix is computed of the differences of the measured values minus the mean values,

$$Z_{ij} = X_{ij} - M_i \qquad \begin{matrix} \text{where } i = 1,2,....6 \\ \text{and } j = 1,2,....N, \end{matrix} \tag{B.4}$$

and the variance-covariance matrix, **S**, of size 6x6, of the control database is computed with elements:

$$S_{ij} = \frac{1}{N-1} \sum_{k=1}^{N} (Z_{ik})\,(Z_{jk}) \qquad \begin{matrix} \text{where } i = 1,2,....6 \\ \text{and } j = 1,2,....6\ . \end{matrix} \tag{B.5}$$

The inverse of the variance-covariance matrix is computed and is used in conjunction with future control measurements to determine if the measurement system remains in a state of statistical control.

C. Procedures for Process Control

At the beginning of an SRM measurement session the features A-0, A-1, B-8, B-9, E-4 and E-5 on the control mask are measured and the multivariate Hotelling's test statistic T^2 is computed as follows:

$$T^2 = \left[\frac{N}{N+1} [Y - M]' \; S^{-1} \; [Y - M] \right] , \tag{C.1}$$

where Y is a vector of newly determined widths and pitches for the above mentioned features.

The system is in control at a 95% confidence level if

$$\frac{(N-6)}{(N-1)6} \; T^2 \leq F_{.05}(6,N-6), \tag{C.2}$$

where the $F_{.05}$ (6,N-6) values are found in table 2. The value (N-6) corresponds to υ in table 2.

At the end of the SRM measurement session, the control is remeasured and the test is repeated. If the system is still in control the SRM data are summarized and a certificate of calibration produced. The value of $((N\text{-}6)/6(N\text{-}1))T^2$ is saved in the control database and the system is ready for the next SRM measurements.

If the test indicates the system is not in control, the data are tagged when they are saved in the control database. The system is then checked to determine the cause of the test failure. A control chart may be used to determine which feature is causing the problem or to see trends in the control data. A control chart for each feature is constructed from the control database as follows:

The mean, $\bar{X}$, and the standard deviation, $\hat{\sigma}$, for each feature are computed using the N repeated measurements from the control database:

$$\bar{X} = \frac{\sum_{i=1}^{N} X_i}{N} \qquad \text{and} \qquad \hat{\sigma} = \sqrt{\frac{\sum_{i=1}^{N} (X_i - \bar{X})^2}{(N - 1)}} \; . \tag{C.3}$$

Control limits are computed by using the following equations:

$$\begin{aligned} &\bar{X} \pm \hat{\sigma}\, t_{.975}(N-1) \text{ for the } 2\sigma \text{ limit} \\ \text{and} \\ &\bar{X} \pm \hat{\sigma}\, t_{.995}(N-1) \text{ for the } 3\sigma \text{ limit.} \end{aligned} \tag{C.4}$$

The values for t are found in table 3. The value $(N - 1)$ denotes degrees of freedom, df, in table 3.

Figure 13 is an example of a control chart of the initial 81 measurements of feature A-0. Future measurements are added to the chart. The control limits remain the same until the process parameters are updated.

If it is determined that the cause of the failure did not affect the SRM measurements (for example, the control photomask was misaligned), the appropriate adjustments are made and the control photomask is remeasured. If the test then shows the process is in control, the SRM data are summarized, a certificate of calibration produced, and the system is ready for the next SRM measurements.

If it is determined that the cause of the failure may also have affected the SRM measurements (for example, the air-conditioning unit malfunctioned during calibration), the SRM must be re-measured after the problem has been corrected and the test indicates the system is once again in control. Major changes to the measurement system dictate reinitialization of the database.

D. Updating Process Parameters

If the measurement system remains unchanged, after collecting a minimum of 30 new (good) sets of control photomask measurements, the process parameters, M, S, and $\hat{\sigma}$ are updated. Equation (B.3) is used to compute M_2, a vector of estimated means for the recently collected control measurements; eqs (B.4) and (B.5) are used to compute S_2, the corresponding variance-covariance matrix; and eq (C.3) is used to compute $\hat{\sigma}_2$, a vector of standard deviations for the repeated measurements for each feature. In the updating process, values that have been flagged as out of control are omitted.

Before updating the control database, a comparison is made between the two databases, the old versus the new, to determine whether or not there is a significant difference in terms of the mean vectors and the variance-covariance matrices. The equivalency of variance-covariance matrices is tested as follows:

$$\text{let} \qquad \ell = N_1 + N_2, \tag{D.1}$$

where N_1 = number of repeated observations in the control database
and N_2 = number of repeated observations in the new set of control observations.

The new control database will contain both new and old measurements.

Let

$$S = \frac{(N_1 S_1) + (N_2 S_2)}{\ell}, \tag{D.2}$$

where S_1 is the variance-covariance matrix of the current control database
and S_2 is the variance-covariance matrix of additional new control measurements.

Compute the statistic [17]:

$$D = 0.5N_1 \text{ trace } [(S_1 - S)S^{-1}]^2 + 0.5N_2 \text{ trace } [(S_2 - S)S^{-1}]^2; \tag{D.3}$$

and test whether:

$$D \leq \chi^2_{df}(0.05).$$

D is distributed as a chi-square random variable with df (degrees of freedom) $= 0.5p(p+1)$ where $p = 6$, the number of features measured. The value of χ^2_{21} (0.05) is 32.67. If $D \leq 32.67$, then the differences between the old and new covariance matrices can be attributed to measurement error at the 95% confidence level. However, if the test fails, ($D > 32.67$),

this suggests that the process has changed in some manner and the cause needs to be identified and evaluated. If the change is significant, appropriate action must be taken and the control process re-initialized.

If the covariance matrices are statistically the same, the means are compared. To do this, first a pooled covariance matrix is computed:

$$S_p = \frac{[(N_1-1)S_1 + (N_2-1)S_2]}{\ell-2}, \tag{D.4}$$

where S_1 and S_2 are defined in (D.2).

Then the statistic is computed:

$$T^2 = \frac{(\ell-p-1)(N_1N_2)}{(\ell-2)p\ (\ell)} (\boldsymbol{M}_1 - \boldsymbol{M}_2)' S_p^{-1}(\boldsymbol{M}_1 - \boldsymbol{M}_2) \tag{D.5}$$

and tested whether:

$$T^2 \leq F_{.05}(p,\ell-p-1)$$

where N_1, N_2 and ℓ are defined in (D.1),
$\boldsymbol{M}_1$ is the mean vector for the current database,
$\boldsymbol{M}_2$ is the mean vector for the newly collected control data,
and $p = 6$, the number of measured features.

T^2 is a random variable with an F-distribution with p degrees of freedom in the numerator and with ℓ-p-1 degrees of freedom in the denominator. The $F_{.05}(p,\ell$-p-1) value is given in table I. If $T^2 > F_{.05}(p,\ell$-p-1), this suggests that there has been a change in the measurement process. The change needs to be identified and appropriate action needs to be taken to reestablish the measurement system and begin the process control anew. However, if $T^2 \leq F_{.05}(p,\ell$-p-1) then the differences between the old and new mean vectors can be attributed to measurement error at the 95% confidence level. Since the test for equality of means was only performed if the hypothesis of equal covariance matrices was not rejected, it can be said that there has been no statistically discernable change in the measurement process at the 90% confidence level and the control may be updated to include the new measurements. The covariance matrix is updated as shown in eq (D.4) and the current covariance matrix is:

$$S = S_p . \tag{D.6}$$

The mean vector is updated as shown below:

$$\boldsymbol{M} = \frac{N_1\boldsymbol{M}_1 + N_2\boldsymbol{M}_2}{N_1 + N_2} . \tag{D.7}$$

The standard deviation for each feature is updated as follows:

$$\hat{\sigma} = \sqrt{\frac{(N_1-1)\hat{\sigma}_1^2 N_1 + (N_2-1)\hat{\sigma}_2^2 N_2}{N_1 + N_2 - 2}} . \tag{D.8}$$

E. Uncertainty Statement for SRM 475

The uncertainties for the certified linewidth and pitch values given in the certificate include small contributions from the measurement precision (random error) and a contribution from the systematic error. The systematic error for both pitch and linewidth values includes a length dependent contribution introduced by correcting the measurements to agree with the NIST Line Scale Interferometer measurements (see sec. 3.5). The systematic error for the linewidth values has a significant contribution (on the order of $\pm$ 0.05 μm) resulting from the edge geometry of the features (see sec. 3.5). See table 1 for a detailed summary of error components.

Before determining the total uncertainty for the reported certificate values, it is assumed that all the measurements on the SRM and in the control database have been corrected to compensate for the difference of measurements between the NIST Line Scale Interferometer System and the optical linewidth measurement system. The correction factor is derived by using the model given below and ordinary least squares to estimate α and its variance:

$$X = \alpha\, Y + \epsilon \tag{E.1}$$

where X represents a measurement from the linewidth measurement system,
Y represents a measurement from the line scale measurement system,
and ϵ is the random error of measurement.

Then the uncertainties, U_L and U_p, for linewidth and pitch measurements are determined by the equations below:

The variance of each SRM measurement, $\hat{s}_j^2$, is

$$\hat{s}_j^2 = \bar{x}_j^2 \frac{\mathrm{var}(\hat{\alpha})}{\hat{\alpha}^2} + \frac{1}{n-1} \sum_{i=1}^{n} (x_i - \bar{x}_j)^2 \tag{E.2}$$

where $\bar{x}_j$ is the average of the jth feature,
$\mathrm{var}(\hat{\alpha})$ is the estimated error of the slope,
$\hat{\alpha}$ is the least squares determination of the slope,
and n is the number of repeated measurements.

The variance of the control measurements, $\hat{\sigma}_k^2$, is

$$\hat{\sigma}_k^2 = \bar{c}_k^2 \frac{\mathrm{var}(\hat{\alpha})}{\hat{\alpha}^2} + CV_k \tag{E.3}$$

where $\bar{c}_k$ is the average of the kth control feature
and CV_k is the kth diagonal element of the variance-covariance matrix for the control data.

Then the pooled variance from the N repeated measurements in the control database and the n repeated measurements of the SRM, $\hat{s}_p^2$, is

$$\hat{s}_p^2 = \frac{(N-1) \sum_{k=1}^{p} \hat{\sigma}_k^2 + (n-1) \sum_{j=1}^{q} \hat{s}_j^2}{(N-1)p + (n-1)q}. \tag{E.4}$$

The uncertainty for pitch measurements is

$$U_p = \pm(1.96\ s_p/\sqrt{n} + \textit{systematic pitch uncertainty})\ \mu\mathrm{m} \tag{E.5}$$

and the uncertainty for linewidth measurements is

$$U_L = \pm(1.96\ s_p/\sqrt{n} + \textit{systematic linewidth uncertainty})\ \mu\mathrm{m}, \tag{E.6}$$

where s_p is determined by using eqs (E.2), (E.3), and (E.4) for pitch and linewidth measurements on the SRM and in the control database. Typically $s_p = .015\ \mu$m and n = 9 repeat measurements. The factor 1.96 converts the uncertainty to the 95% confidence level.

ACKNOWLEDGMENTS

The authors thank Susannah Schiller for suggesting the statistical tools to assure process control of the linewidth SRM measurement system and for her review of this documentation.

REFERENCES

[15] Croarkin, C., Measurement Assurance Programs Part II: Development and Implementation, Natl. Bur. Stand. (U.S.) Spec. Publ. 676-II, 1985, pp. 35.

[16] Anderson, T.W., "An Introduction to Multivariate Statistical Analysis," Second ed. John Wiley and Sons, 1984. Chapter 5, pp. 156-190.

[17] ibid., p. 423.

Table 2. Critical Values of $F_{.05}(6,\nu)$ of the F–Distribution

ν	$F_{.05}(6,\nu)$
10	3.217
12	2.996
14	2.848
16	2.741
18	2.661
20	2.599
22	2.549
24	2.508
26	2.474
28	2.445
30	2.421
32	2.399
34	2.380
36	2.364
38	2.349
40	2.336
42	2.324
44	2.313
46	2.304
48	2.295
50	2.286
52	2.279
54	2.272
56	2.266
58	2.260
60	2.254
62	2.249
64	2.244
66	2.239
68	2.235
70	2.231
72	2.227
74	2.224
76	2.220
78	2.217
80	2.214
82	2.211
84	2.209
86	2.206
88	2.203
90	2.201
92	2.199
94	2.197
96	2.195
98	2.193
100	2.191
102	2.189
104	2.187
106	2.185
108	2.184
110	2.182
112	2.181
114	2.179
116	2.178
118	2.176
120	2.175
∞	2.099

Table 3. Critical Values of $t_{.975}(df)$ and $t_{.995}(df)$ of the Student's t Distribution

df	$t_{.975}$	$t_{.995}$
10	2.228	3.169
12	2.179	3.055
14	2.145	2.977
16	2.120	2.921
18	2.101	2.878
20	2.086	2.845
22	2.074	2.819
24	2.064	2.797
26	2.056	2.779
28	2.048	2.763
30	2.042	2.750
32	2.037	2.738
34	2.032	2.728
36	2.028	2.719
38	2.024	2.712
40	2.021	2.704
42	2.018	2.698
44	2.015	2.692
46	2.013	2.687
48	2.011	2.682
50	2.009	2.678
52	2.007	2.674
54	2.005	2.670
56	2.003	2.667
58	2.002	2.663
60	2.000	2.660
62	1.999	2.657
64	1.998	2.655
66	1.997	2.652
68	1.995	2.650
70	1.994	2.648
72	1.993	2.646
74	1.993	2.644
76	1.992	2.642
78	1.991	2.640
80	1.990	2.639
82	1.989	2.637
84	1.989	2.636
86	1.988	2.634
88	1.987	2.633
90	1.987	2.632
92	1.986	2.630
94	1.986	2.629
96	1.985	2.628
98	1.984	2.627
100	1.984	2.626
102	1.983	2.625
104	1.983	2.624
106	1.983	2.623
108	1.982	2.622
110	1.982	2.621
112	1.981	2.620
114	1.981	2.620
116	1.981	2.619
118	1.980	2.618
120	1.980	2.617
∞	1.960	2.576

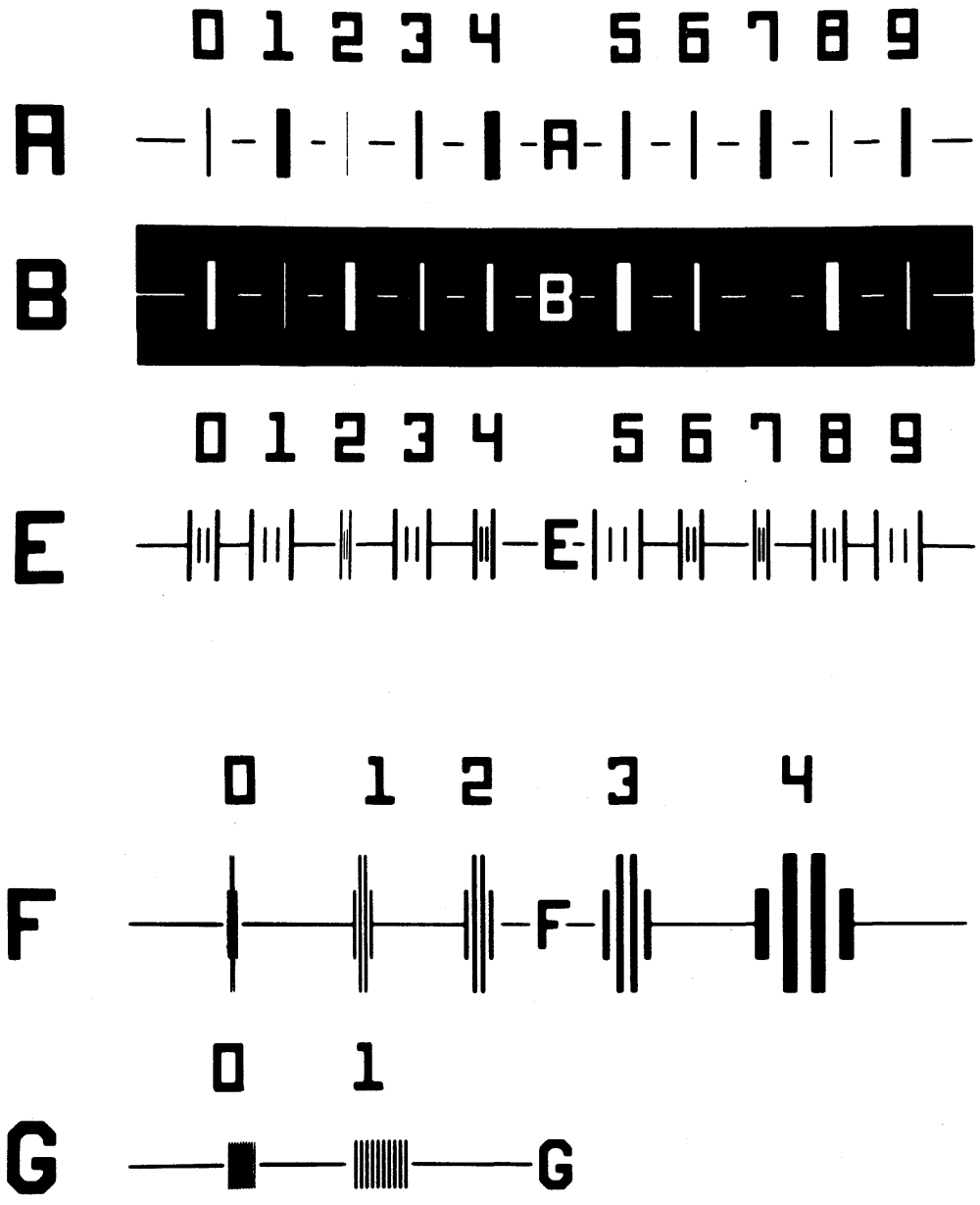

Figure 12. A view of the basic pattern on the SRM 475 control photomask. Features 0 and 1 in row A, 8 and 9 in row B, and 4 and 5 in row E are measured before and after each SRM is calibrated. Features 4 and 5 in row E and feature 1 in row G have been independently calibrated on the NIST Linescale Interferometer by the NIST Dimensional Metrology Group.

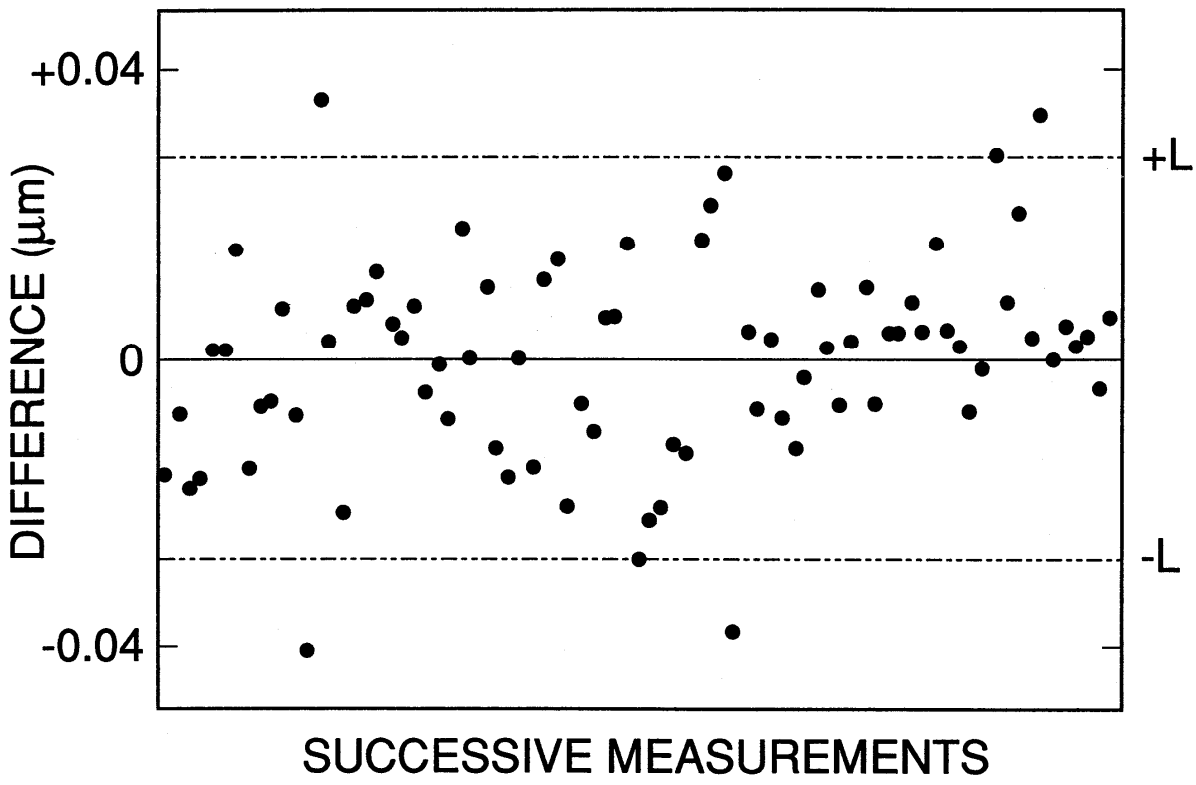

Figure 13. Control chart of feature A-0. Line M is the mean; and lines L mark 95% confidence level. The chart includes the first 81 measurements of the feature. Future measurements are added to the chart.